University of Southern Queensland

School of Engineering

Using non-synchronous generation with grid forming ability to improve the response time during a system restart of the Queensland Electricity Network

A dissertation submitted by

Stephen John Connor

in fulfillment of the requirements of

ENP4111 Professional Engineer Research Project

towards the degree of

Bachelor of Engineering Honours

2024

This page intentionally left blank

University of Southern Queensland

School of Engineering

ENP4111 Dissertation Project

(This is a 2-unit research project in Bachelor of Engineering Honours Program)

Limitations of Use

The Council of the University of Southern Queensland, its Academic Affairs, and the staff of the University of Southern Queensland, do not accept any responsibility for the truth, accuracy or completeness of material contained within or associated with this dissertation.

Persons using all or any part of this material do so at their own risk, and not at the risk of the Council of the University of Southern Queensland, its Faculty of Health, Engineering and Science or the staff of the University of Southern Queensland.

This dissertation reports an educational exercise and has no purpose or validity beyond this exercise. The sole purpose of this dissertation project is to contribute to the overall education within the student's chosen degree program. This document, the associated hardware, software, drawings, and other material set out in the associated appendices should not be used for any other purpose: if they are so used, it is entirely at the risk of the user.

CERTIFICATION

I certify that the ideas, designs and experimental work, results, analyses and conclusions set out in this dissertation are entirely my own effort, except where otherwise indicated and acknowledged.

I further certify that the work is original and has not been previously submitted for assessment in any other course or institution, except where specifically stated.

Student Name **Stephen John Connor**

Student Number: [redacted]

Signature

28th October 2024

Date

ABSTRACT

The need to perform a full restart of the Queensland Electricity Network is rare but with the move to more Distributed Energy Resources (DER) the need to have new way to provide restart services is needed.

By utilising DER spread throughout the Queensland Electricity Network away from traditional generation sources, Distributed Restart Zones (DRZ) will be able to provide enough restart services to shorten the time it takes to completely restart the Queensland Electricity Network.

The ability of a DER such as solar, wind, or batteries to provide a restart service is limited to their ability to provide the service when needed. With DRZs, it should be possible to start with one DER in a location and grow the DRZ (Microgrid) to include several different DERs to be able to support each other.

The following research investigates the use of a Battery Energy Storage System (BESS) as the DER to provide the restart service by using a simulated model of a Grid Forming Inverter (GFMI), to create a DRZ modelled on a real-world situation. The response of the inverters is evaluated for suitability of a BESS to provide the restart service with initial results being mixed. Further investigate using a different GFMI control system is needed.

ACKNOWLEDGEMENTS

I would like to express my gratitude to my academic supervisor, Associate Professor (Electrical Engineering) Tony Ahfock, for his support, guidance and encouragement through my research. His feedback and constructive criticism have been invaluable in shaping this dissertation.

I would also like to extend my thanks to my industry supervisor Matthew Zillmann (Energy Queensland, Principal Engineer – Connections Assessment), for his support and guidance throughout this research. His practical insights and expertise have been invaluable in the successful completion of this research.

And finally, I am profoundly grateful to my family for their unwavering support and encouragement throughout this journey. I am deeply grateful to my partner, Annette, for her love, patience, and unwavering belief in my abilities.

TABLE OF CONTENTS

LIST OF TABLES

LIST OF FIGURES

GLOSSARY

AEMO	Australian Energy Market Operator
APC	Active Power Controller
AVSG	Adaptive Virtual Synchronous Generator
BESS	Battery Energy Storage System
BS	Black start
BSG	Black start generation
CB	Circuit Breaker
DER	Distributed Energy Resources: generation or storage assets that are not centrally controlled by AEMO dispatch
DNSP	Distributed Network Service Provider
DRZ	Distributed Restart Zone
EPRI	Electric Power Research Institute
ESCRI	Energy Storage for Commercial Renewable Integration
ESO	Energy System Operator
ESS	Energy Storage System
GDC	Generalised Droop Controller
GFLI	Grid-Following Inverter
GFMI	Grid-Forming Inverter
HV	High Voltage
HVDC	High Voltage Direct Current
IBR	Inverter Based Resource
IEEE	Institute of Electrical and Electronics Engineers
kVAR	kilovolt amps reactive
kW	kilowatts
MW	Megawatts
NEM	National Electricity Market
NDA	Non-Disclosure Agreement
OEM	Original Equipment Manufacturer

OWF	Offshore Wind Farm
PCC	Point of Common Coupling
RPC	Reactive Power Controller
PSH	Pumped Storage Hydro
PWM	Pulse Width Modulation
RMS	Root Mean Squared
RoCoF	Rate of Change of Frequency
SG	Synchronous Generator
SM	Synchronous Machine
SRAS	System Restart Ancillary Services
SRS	System Restart Service
TNSP	Transmission Network Service Provider
TOV	Temporary Overvoltage
VISMA	Virtual Synchronous Machine
VRB	Vanadium Redox battery
VSG	Virtual Synchronous Generator
WF	Wind Farm

CHAPTER 1 INTRODUCTION

The need to perform a full restart of the Queensland Electricity Network is rare and relies on existing coal fired power stations to provide a top-down restart. It requires restart services to be located close to power stations, which are located in Central and Southern Queensland, and can take over 24 hours to energise the entire state.

> *"The continued security of the power system, at the lowest cost to consumers, is possible only if sufficient black start sources are in place. Without such a capability there is no guarantee that the power system can fully recover even within days after a major supply disruption." (Aurecon, 2021)*

With the move to more regionalised non-synchronous generation such as solar, wind, hydro and batteries in the grid, the provision of restart services incorporating these generators is a problem that needs a solution now.

1.1 Aim

This research investigates if non-synchronous generation with grid forming ability can improve the response time of a black system restart of the Queensland Electricity Network. It investigates a bottom-up system restart with the creation of Distributed Restart Zones (DRZs) to run in parallel with the standard top-down system restart. By creating DRZs centred around distributed energy resources (DER) with grid forming ability, it is expected the total restoration time of the Queensland Electricity Network will be reduced.

1.2 Objectives

1. **Understanding the state of current Queensland Electricity Network**: Analyse the current state of the Queensland Electricity Network, its generation sources, and its load

profiles. This will involve a detailed study of synchronous and non-synchronous generators currently in use.

2. **Technical Evaluation of Grid Forming Inverters (GFMIs)**: Conduct a comprehensive review of grid forming inverters, their operation, and their benefits. This will include studying their ability to provide voltage and frequency support, and their performance under different network conditions.

3. **Integration of Non-Synchronous Generation**: Investigate the potential for integrating more non-synchronous Inverter Based Resources (IBRs) into the grid, such as wind and solar power. This will involve studying the impact of these sources on grid stability and reliability.

4. **Grid Stability Analysis**: Perform a stability analysis of the grid with increased penetration of non-synchronous generation and grid forming inverters. This will involve simulations or modelling to predict the behaviour of the network under different scenarios.

5. **Regulatory and Economic Considerations**: Examine the regulatory implications of increasing non-synchronous generation and using grid forming inverters. This might also involve an economic analysis to understand the cost-effectiveness of these technologies.

6. **Development of Recommendations**: Based on the findings, develop recommendations for policy makers, grid operators, and other stakeholders on how to effectively integrate these technologies into the Queensland Electricity Network.

1.3 Outcomes and benefits

The use of grid-forming inverter-based resources for black start capability in the Queensland Electricity Network could have several potential outcomes and benefits:

1. **Improved Black Start Capability**: Grid-forming IBRs can provide black start capability, which is the ability to restart the power grid after a blackout without relying on external power. This could significantly improve the resilience of the Queensland Electricity Network.

2. **Increased Grid Stability**: Grid-forming IBRs can help maintain voltage and frequency stability during the black start process. This could lead to a smoother and faster recovery from blackouts.

3. **Integration of Renewable Energy Sources**: Grid-forming IBRs can enable the integration of renewable energy sources like wind and solar power into the black start process. This would reduce reliance on fossil fuel-based power plants in the black start process.

4. **Cost Savings**: By improving the efficiency and speed of the black start process, grid forming IBRs could potentially lead to cost savings in the long run.

5. **Regulatory Compliance**: Implementing grid-forming non-synchronous IBRs for black start capability could help the Queensland Electricity Network comply with future regulatory requirements related to grid resilience and renewable energy integration.

1.4 Chapter Overview

Chapter 2 investigates the background to the issue and what research has been conducted to date. There has not been much research undertaken investigating the use of non-synchronous generation as a restart service in Queensland.

Chapter 3 outlines the methodology used to investigate the use of Battery Energy Storage Systems (BESS) as a restart service on the Queensland electricity network. The test cases look at a real-world situation and how the network could be energised.

Chapter 4 contains the results of the test cases. Initial investigation shows that the GFMI control system used is not sufficient to prevent power swings when energising a load that includes transformers and short transmission lines.

Chapter 5 is the conclusion where the original objectives are revisited and assessed to see if they were met. It also includes a summary of future work that is suggested.

CHAPTER 2 BACKGROUND AND LITERATURE REVIEW

Even though it has only happened three times over the last 60 years, in South Australia in 2016, Northern Queensland in 2009, and New South Wales in 1964 (AEMC, 2016), black system restarts on the National Electricity Market (NEM) do occur, with restoration of the affected network taking from many hours up to several days to complete the restoration.

The GPST Blackouts and System Restoration Research report (2021) produced by Aurecon, delves into possible factors that may cause a major disturbance large enough that the frequency and voltage on the network cannot be maintained. These factors such as, aging assets (coal fired power stations), aging network assets (poles and wires), increasing impact of global warming, increasing occurrences of cyber-attacks, and increasing possibility of electrical system failures due to IT system failures mean that there could be a real possibility of the need for more black system restarts in the future.

Current black system restarting of an electricity network is similar throughout the world. As most synchronous generators (e.g. coal fired synchronous generators) are unable to start themselves, some external form of generation is needed to provide enough energy back into the network to enable their restart. Australia uses the same method of system restart as the UK which has "*remained largely unchanged for many years and is based on a transmission-led approach of starting large synchronous generators, energising a skeleton transmission network, and controlling demand"* (National Grid ESO, 2019).

Aurecon 2021 states that there are numerous requirements that are sought from a black start generator, with this research focussing on the following points:

- Start-up independent of external supplies and without drawing power from the network.

- Energise parts of the transmission and distribution networks.
- Provide steady-state and dynamic frequency and voltage control during the restoration process and its early stages.
- Provide steady-state and dynamic voltage control. For early stages of restoration this may include providing all the reactive power needed for energising transmission lines, transformers and starting loads (such as auxiliary motors of other non-black start generators).
- Maintain a level of supply for a minimum time as agreed with the system operator.

"Grid-Forming (GFM) inverters are gaining popularity for their ability to replicate the dynamics of synchronous generation" (Smith., et al, 2022).

With the increased number of distributed energy resources and the reduction in the amount of traditional synchronous generation, the traditional top-down restoration of electricity network is changing. In top-down restoration plans, the black start units are utilised to energise the transmission network, whereas in bottom-up plans, the black start units are used to energise the sub-transmission network (Asheibi and Shuaib, 2019).

While there has been some investigation into using non-synchronous Inverter Based Resources (IBR) for black start system restoration (Aurecon, 2023), this was primarily for top-down system restart.

2.1 Literature review

2.1.1 Introduction

With the increasing connection of non-synchronous Inverter Based Resources (IBR) to the National Electricity Market, restoring power following a major disruption will become increasingly difficult.

This literature review examines the process of a black system restart and evaluates the potential of Distributed Energy Resources (DER) to provide black start services. Additionally, it investigates GFMIs, and their control methods to assess the viability of non-synchronous generators for black restart services in Queensland.

2.1.2 Established knowledge

Black system restart of an electricity network has been studied extensively, from the development by Zhu et.al (1991) of a new graphical interface to assist operators during power system restoration, through to the many studies on the use of IBRs for black start such as *Blackstart of Power Grids with Inverter-Based Resources* (Jain, et.al. 2020) and *The Role of Inverter-Based Resources During System Restoration* (Aurecon, 2023).

Traditionally, a black start involves using ancillary services to provide power to non-black start generators (steam turbine units) for cranking power. These ancillary services have previously been provided by black start generators such as hydroelectric, diesel, and gas turbine generating units (Sun, 2011).

From the Queensland Energy Map, Figure 1, (Queensland Department of Energy and Public Works, 2021), there is currently approximately 8.1GW of aging coal fired synchronous generators and 5.2GW of DER connected to the National Energy Market (NEM), Figure 2.

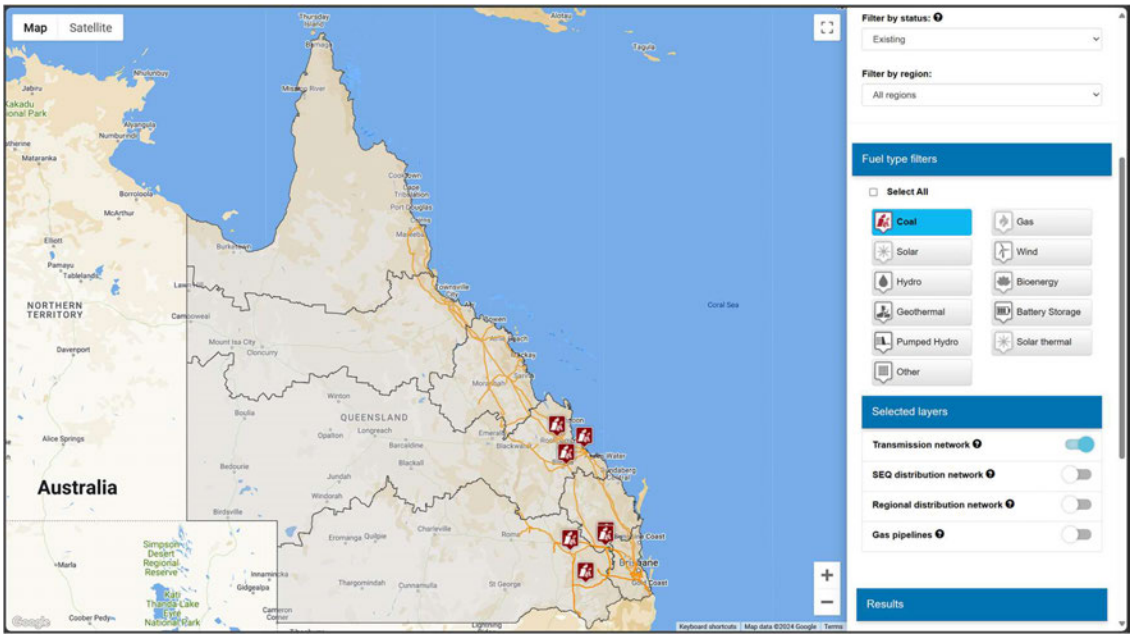

Figure 1 - Existing Coal fire synchronous generators. Queensland Department of Energy and Public Works (2021).

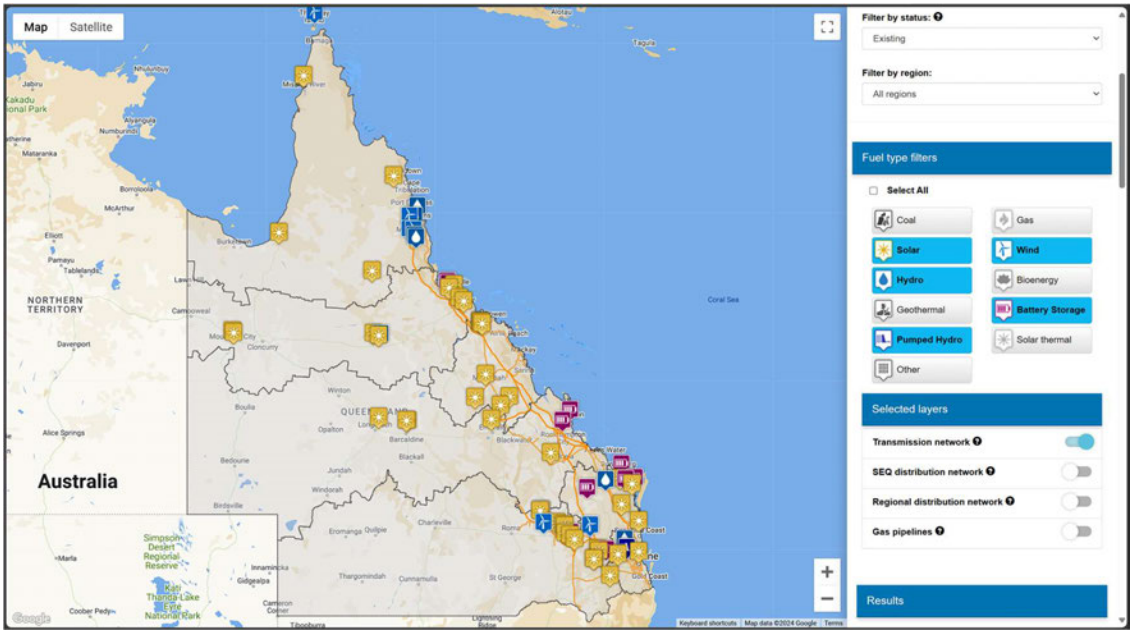

Figure 2 - Existing Distributed Energy Resources. Queensland Department of Energy and Public Works (2021).

There is also currently 3.5GW of DER under construction, Figure 3, with another 74.8GW of DER proposed, Figure 4.

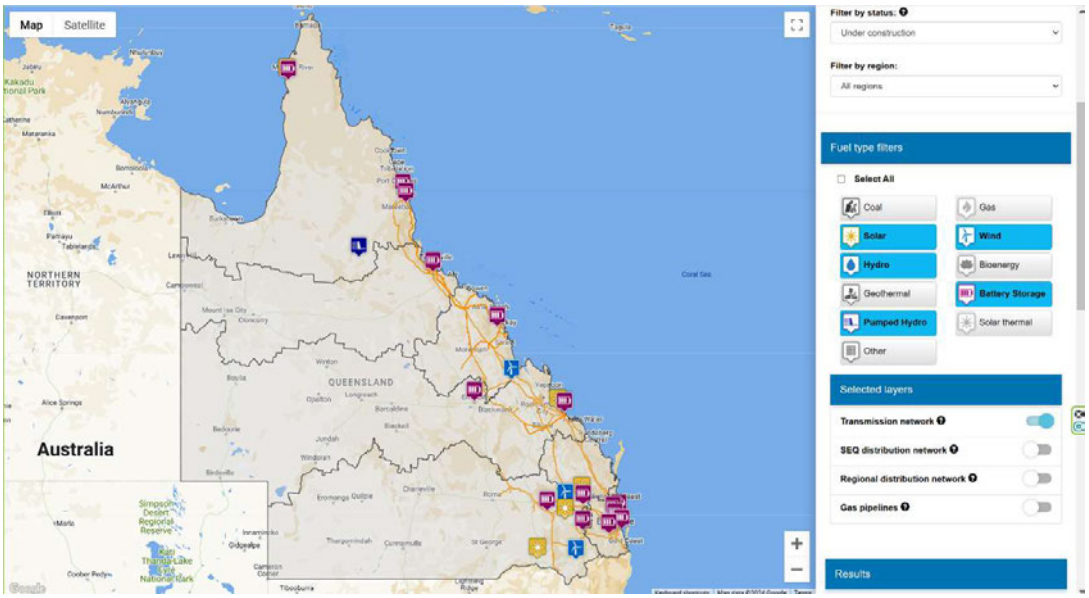

Figure 3 - Under construction Distributed Energy Resources. Queensland Department of Energy and Public Works (2021).

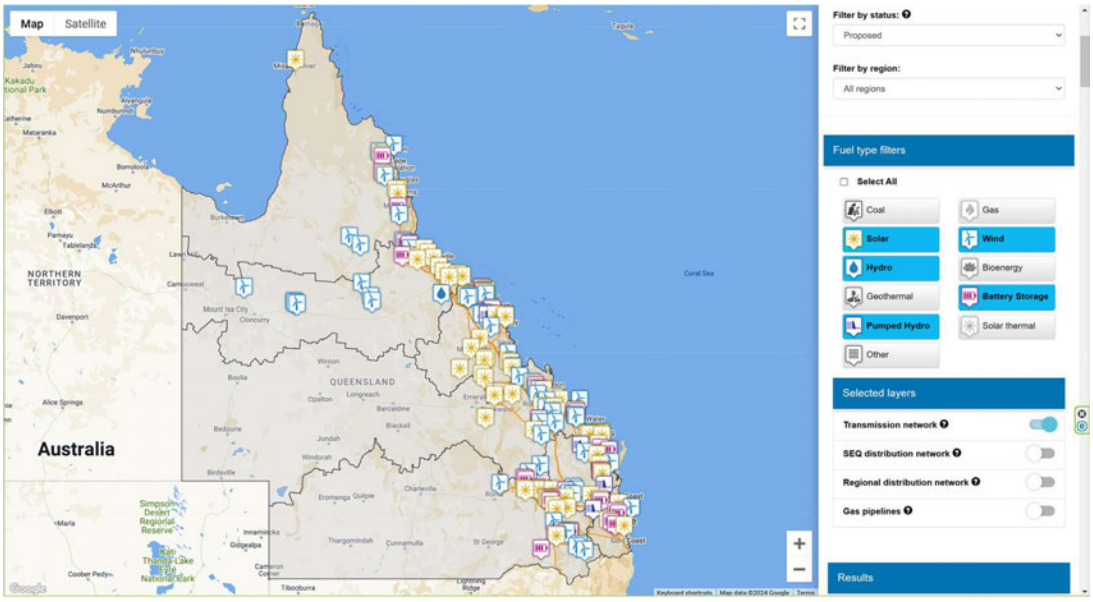

Figure 4 - Proposed Distributed Energy Resouces. Queensland Department of Energy and Public Works (2021).

With the increased connection of DERs to the NEM and the reduction in the amount of traditional synchronous generation, the traditional top-down restoration of electricity network is changing. In top-down restoration plans, black start units are utilised to energise the transmission high voltage system, whereas in bottom-up plans, the black start units are used to energise the sub-transmission or distribution high voltage system (Asheibi and Shuaib, 2019).

Any generation that is used as a black start service in Australia is required to comply with the System Restart Ancillary Services from AEMO (2021a). These technical requirements are to ensure that any black start service is able to start by itself, provide (and dynamically control) the network voltage required as specified by Australian Energy Market Operator (AEMO), and control power system frequency as required by AEMO.

The Application of Advanced Grid-scale Inverters in the NEM whitepaper produced by AEMO (2021b) discusses the challenges facing the NEM with the increased connection of IBRs. Section 3.4 of the whitepaper (AEMO 2021b) investigates the application of using IBRs as a system restart with three case studies discussed in the Battery Energy Storage, Wind Energy, and Other sections. The key finding of the whitepaper's investigation of the ability of IBRs to provide system restart capability was that grid-forming inverters have the potential to support or even initiate system restart, however this has yet to be demonstrated at scale.

2.1.3 Black start with Grid-Forming Inverter-Based Resources

With the increasing penetration of IBR such as wind, photovoltaic (PV), and BESS units there is more research being done to understand the technical potential and associated costs of using grid-forming resources to provide black-start support (Jain., et.al., 2020).

While the research conducted by many has assessed the feasibility to use grid-forming IBRs for black start support, little attention has been given to some additional concerns such as:

1. addressing the increased risk associated with the stochasticity of wind and solar PV based IBRs;
2. evaluating the ability of protective relays on the restoration path to operate reliably during a black start in view of the limited short-circuit current capability of IBRs;
3. understanding the impact that IBRs might have on black-start criteria, such as the minimum time for which a black-start resource must provide rated power; and
4. modelling and simulation to understand the performance of IBRs for a black start.

What is a grid-forming inverter?

As there is no international standard definition as to what a grid-forming inverter is, for the purpose of this research, the AEMO definition in the Voluntary Specification for Grid-Forming Inverters (AEMO, 2023) will be used.

> *A grid-forming (GFM) inverter maintains a constant internal voltage phasor in a short time frame, with magnitude and frequency set locally by the inverter, thereby allowing immediate response to a change in the external grid. On a longer timescale, the internal voltage phasor may vary to achieve desired performance.*

Much, if not all, of the current research is being done using simulations. The simulations such as those conducted in Jain, et.al, (2020) used simplified simulation to investigate the feasibility of using IBRs as part of a restart plan. This research used MATLAB SIMULINK/Simscape to simulate the start of a 1.5MW motor with the behavioural model of a current limited, grid forming inverter in 4 configurations.

a) On site kick starter for a black start
b) Remote kick starter for a black start

c) Fully functional black start resource

d) A collective black start

This is a limited study that requires further investigation on the inverter modelling, motor modelling, better modelling of the 4 configurations, and protective relay modelling.

Aurecon (2023) performed more Australian specific simulations as part of the report "The Role of Inverter-Based Resources During System Restoration". These simulations were conducted using PSCAD with models obtained from Original Equipment Manufacturers (OEM)s with a Non-Disclosure Agreement (NDA) being required between Aurecon and the OEMs. The black start scenarios that Aurecon investigated were grid-forming BESS, synchronous generator, and grid-following BESS with a synchronous condenser connected on the network. The simplified network also consisted of protection (distance and differential), transmission lines, and load. While these are more specifically Australian scenarios, it still uses a simplified simulation.

National Grid ESO conducted a multi-year project to investigate the role that IBR and DER can play in the black restart of a national electricity network. The initial work was done with modelling and simulations carried out using PowerFactory. The research by National Grid ESO then progressed to live trials in three parts. These trials were:

- Trial 1
    - Hydro generator DER
    - Energising a mixture of substation and transmission line assets
- Trial 2
    - Biomass DER
    - Energise a mixture of substation and transmission line assets
- Trial 3

- BESS DER in conjunction with a prototype Distributed Restart Zone Controller
- Energise a mixture of substation and transmission line assets

2.1.4 Distributed Energy Resources as a restart service

Wind energy as the DER

Pagnani, et.al (2020a) research reviewed the ongoing research on Black Start (BS) service integrated with Offshore Wind Farms (OWFs). They looked at grid forming strategies including BESS to perform the role of Black Start Generators (BSG) to energise the submarine cable from onshore to the OWF. It was simulated with PSCAD/EMTDC as during BS an OWF can go through switching transients, inrush currents, system resonance, and over voltages.

Pagnani et.al (2020b) also suggests in their "Overview of Black Start Provision by Offshore Wind Farms" research that by using a decentralised GFM BESS, a smaller BESS connected directly at the OWF offers higher reliability as the failure of one BESS located at the offshore wind turbines, does not prevent the entire system to restart the onshore network under black start conditions. While Pagnani, et.al investigated different grid-forming technologies related to OWF, they did not research how the modelled simplified circuit would react if it was part of a larger network.

Liu and Liu (2019) found in their research the ESS needs to be of sufficient size to enable a wind farm to be useful for black start. The BESS sized needs to be large enough to supply the auxiliary power to the wind farm turbine for yaw and pitch control, be able to assist with frequency response as the non-black start generators start up, and be able to deliver real and reactive power when required during the black start. Again, this is just a simulation and does not look at the interaction and performance of a larger network during a black start with a wind farm and BESS.

Case study 4 in AEMO (2021b) investigated the use of a 69MW wind farm in Scotland that conducted grid-forming trials in 2019. These trials explored different control system tunings with the results showing that the response to actual and artificial grid disturbances (except for the largest disturbances), including a black start event, was similar to synchronous generators of a similar size. The trials also found that DERs could play a part in the re-energisation process with the grid-forming wind farm proven to be able to provide system restart and potentially bringing distribution customers online faster than a top-down process.

Solar as the DER

Research conducted by Tongge et.al. (2020) confirms that a PV-BESS configuration on a simulated network can be used as a black start power supply. The researchers used the PV-BESS not only as a black start unit, but also to regulate the frequency and voltage during the black start. The Dijkstra algorithm was used to divide the IEEE39 node system example into clusters so that the independent network clusters could be restarted in parallel improving the black start time. While this research has proven that PV-BESS configuration in independent clusters can improve the restart time, it has only used a IEEE39 node system example that does not consider specific real-world conditions.

Li, et.al. (2019) also confirm that a PV-BESS configuration can be utilised as a black start unit, but they noted the issue of variability of the PV output power. To minimise this issue, their research paper developed an optimisation strategy that analyses the required power for a black start on the network, predicts the amount of PV-BESS power available, optimises the control strategy for the PV-BESS black start, and then schedules the output of the PV-BESS as required. In theory this is promising and the simulations that were verified for sunny, cloudy, and rainy days show the black start using PV-BESS units is feasible except for rainy days. The effects of load input and fluctuation of PV on voltage and frequency were not considered.

The ability to black start using PV power plants without BESS was confirmed through simulations as feasible by Feldman and Vasques de Oliviera (2021) and Asensio et.al. (2023). Both investigated the ability of a PV power plant to supply the required voltage, current, and reactive and active power need for black start capability. This is also promising but again these were only simulated on a simple network without investigating the PV power plant response on a larger, more complex network.

Hydro as the DER

There has been little research into the use of pumped storage hydro (PSH) and their black start capability. Gracia et al. (2019) suggest that a hydroelectric generator is suitable for black start if there is a large enough black start generator onsite that can supply the auxiliary power for

- Oil pumps for the bearing lubrication system and for the governor to move the wicket gate, air compressors, and field excitation coils.
- Short starting time.
- Sufficient real power capability
- Sufficient reactive power capability
- Frequency support

While PSH units have almost all the advantages of conventional hydro units, there is an issue where the water in the upper storage may have been depleted during normal market dispatch and therefore some water would always have to be held in reserve.

HVDC Links

Case study 4 in the paper from AEMO (2021b) is a study presented by The National HVDC Centre and Electric Power Research Institute (EPRI) on a simulated black start using a

1400MW HVDC connection between Norway and Scotland. The simulation started with the energisation of the HVDC station on the Scottish side before energising the surrounding HV feeders which then enabled a hydro power plant to come online (Adeui, 2020). In the simulation, a soft start is where the HVDC station ramps up the voltage to reduce in rush current to the transmission transformers.

There are only a few HVDC connections in Australia, with Directlink being the only one that connects the QLD NEM to the NSW NEM. Directlink is a 180MW HVDC link between Bungalora and Mullumbimby in New South Wales and while it is wholly located in NSW, it provides a link in the Southeastern corner of QLD (APA, 2024). As this is a transmission connection, if assessed as a possible black start, it would assist in a top-down restart and will not be considered further in this research.

Battery energy storage as the DER

The literature review so far has resulted in very few studies into using just a BESS for a black system restart with only one found that investigated the suitability of a vanadium redox battery (VRB) (Dong et.al 2014). This research did not investigate a system restart from a complete black system, but from the VRB islanding itself and creating a microgrid. This microgrid was then able to restore supply to load within the microgrid area and was then able to resynchronise to the normally restarted network.

Izadkhast et.al (2022) simulated two scenarios with different types of loads connected at various times. The research mainly investigated the response of a proposed novel three-mode controller. The research simulations found that at a certain point of the black start, when additional load was added, the voltage and frequency dropped significantly due to the inrush current of the load being energised. It is mentioned that the simulated loads were modelled as directly "*connected to the grid with no power-electronic interface in-between the induction*

machine and the islanded area". If these were modelled as a real-world situation, the inrush current would be much less resulting in a better voltage and frequency response. The simulations were performed in MATLAB SIMULINK and found that with the proposed novel controller the modelled BESS was able to restore the micro-grid step-by-step (even with DER connected) while maintain the voltage and frequency within the required limits.

Case study 3 appearing in AEMO (2021b) has been adapted from a CIGRE paper (Cherevatskiy et al, 2020) that investigated the ability of the Dalrymple Energy Storage for Commercial Renewable Integration (ESCRI) BESS located in South Australia, Figure 5, to perform as a black start service. This GFM BESS was found to be able to provide black start services to the local 33kV distribution network but was unproven beyond this local distribution network.

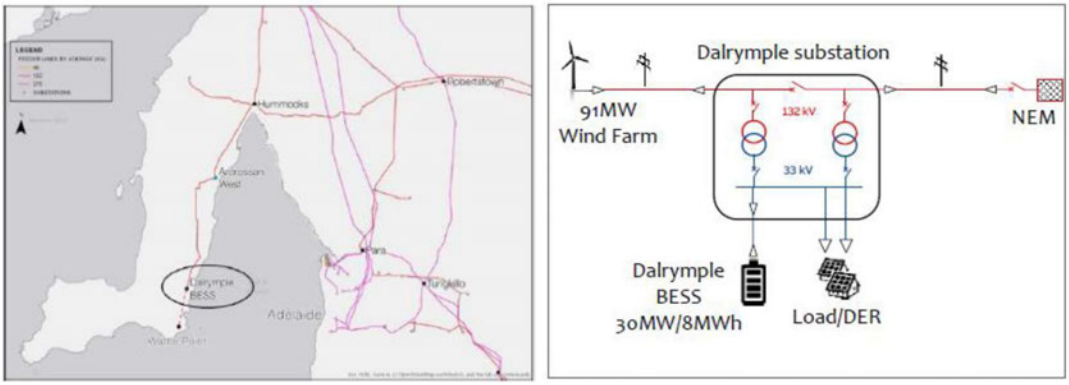

Figure 5 - ESCRI battery network location - a simple network diagram (Cherevatskiy et al, 2020)

The reenergisation of the distribution network was achieved by using a soft energisation of the BESS transformers, one substation transformer and two 33kV distribution feeders. This soft energisation involved slowly ramping up the voltage to reduce inrush current and harmonics with the results in Figure 6.

Figure 6 - Left - Ramp-up of voltage by the GF-BESS to soft energise transformers; Middle - Resulting currents are so small they were not captured by the high-speed recorder; Right - active and reactive power profiles for energisation of 33kV feeders.

Grid-forming inverter control methods

Control of a GFMI needs to mimic a conventional synchronous generator to control voltage, current and frequency, and be able to respond to system disturbances.

As Rathnayake et al. (2021), Unruh, Nuschke, Strauß & Welck (2020), and Lin et al. (2020) report, control methods generally fall into three categories. These are droop-based, synchronous machine based, and other.

Droop control is the most well-established grid-forming method of inverter control which was first proposed in the early 1990s (Lin et al., 2020). Rathnayake et al. (2021) then splits droop control into additional control structures which are Frequency-based droop, Angle-based droop, and Power Synchronisation Control (PSC).

Synchronous Machine based control was developed to deal with shortcomings of the droop controllers lack of inertia support (Rathnayake et al., 2021). Within the synchronous-machine-based control group of GFMI control methodologies they can be spilt into control systems with three of the most popular being VISMA (Virtual Synchronous Machine), Swing equation emulation, and Augmented Virtual Synchronous Generator (VSG) control.

The VISMA model is based on a two-shaft synchronous machine model with active and reactive power controlled based on the virtual torque and virtual excitation base on the measured voltage at the Point of Common Coupling (PCC).

Swing equation control uses a swing equation that represents the rotor side dynamics of a synchronous machine. A key advantage using swing equation control is that the damping constant and the moment of inertia can be changed during operation to improve the response of the GFMI.

Augmented VSG control provides better damping, improved transient stability, and a better transient response. The Augmented VSG control can be modified to further improve its operation by combining features from other controllers. As mentioned in Rathnayake et al. (2021), by incorporating a generalised droop controller (GDC) based on VSG it guarantees a desired Rate of Change of Frequency (RoCoF) in standalone mode.

Other methods including Virtual oscillator based and ViSynC will not be covered as a control system in this research.

2.1.5 Knowledge gap

Non-synchronous generation for black start

The ability to use non-synchronous grid forming units for black start is being investigated worldwide. AEMO (2021) states the use of asynchronous generation in the System Restart Ancillary Services (SRAS) Guideline, but there has been minimal specific research undertaken on the use of non-synchronous grid forming units as System Restart Services (SRS) on the Queensland Electricity Network. Section 5.2 of the GPST Blackouts and System Restoration Research Final Report (2021) states

"*Furthermore, the use of IBRs during system restoration is very limited in system restart plans."*

The research that has been conducted thus far has been on several different DERs with and without energy storage. There has been no research that I am aware of that simulates a black start with several different DERs connected in the same network to investigate the response.

While there has been some research conducted into using IBR for black start system restoration (Aurecon, 2023), these are primarily top-down system restart studies. The research in this dissertation will investigate what role IBRs can play in a bottom-up or distribution level system restart in parallel with a top-down system restart. While there has been some research conducted on the Australian Electricity Transmission Network, there has not been any research conducted to investigate the creation of Distributed Restart Zones (DRZs) on the Queensland Electricity Distribution Network.

As AEMO (2021b) states, "*For IBR that is connected via the distribution network, a bottom-up approach could be used. This would involve energising distribution load first, before energising up the transmission network to larger generators"*. The simulations in this research will investigate this exact bottom-up approach using real world data.

2.1.6 Conclusion

The literature review has shown that grid-forming IBRs can provide a black start service where some forms of DER are more suited as the generation source. While there has been some simulation and real-world testing of the ability to use DERs with GFMIs worldwide, there has only been limited research into the ability of GFMIs to provide a bottom-up black restart service in Queensland to support a top-down system restart.

For this research, the most likely DER to be used by the Distribution Network Service Provider (DNSP) as a bottom-up black restart service is a BESS, due to the number of these units currently being constructed and able to be directly controlled by the DNSP. The ability of the DNSP to directly control the BESS means they will have the ability to provide the support needed if conducting a bottom-up system restart in conjunction with a top-down system restart of the Queensland Electricity Network.

CHAPTER 3 METHODOLOGY

Grid-forming inverter control.

As each manufacturer has their own proprietary control system, it is difficult to know exactly what method of control they utilise. To enable simulation of a GFMI a digital twin model is needed to investigate the system response when energising various parts of the network. In lieu of a digital twin model, a simple GFMI model was researched and created.

3.1 Simulation of models

Simulation of synchronous machines

The model simulation of a synchronous machine in SIMULINK follows the IEEE Guide 1110-2019 for Synchronous Generator Modelling Practices and Parameter Verification with Applications in Power System Stability Analyses. This approach uses the direct-quadrature axis analysis that simplifies the analysis of synchronous machines. Figure 7 shows the electrical model of a synchronous machine in the d and q frame, with Figures 8 and 9 showing the d-axis and q-axis equivalent circuits.

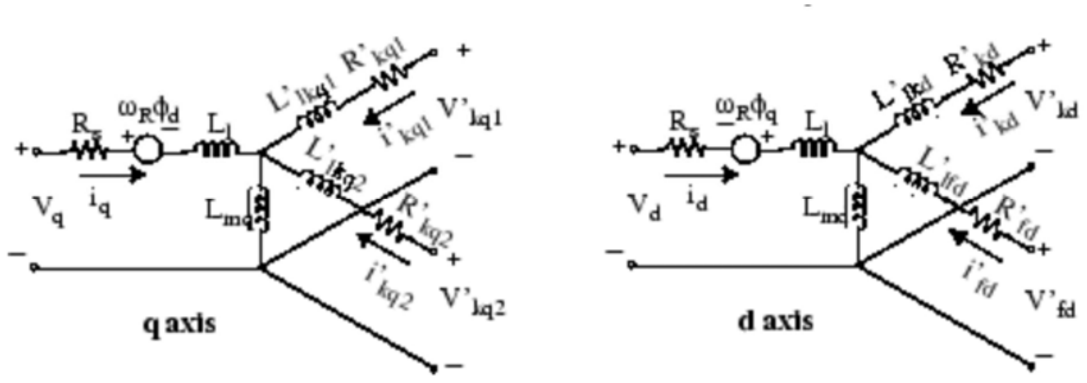

Figure 7 - Electrical model of a synchronous machine in dq frame. Matlab 2024b.

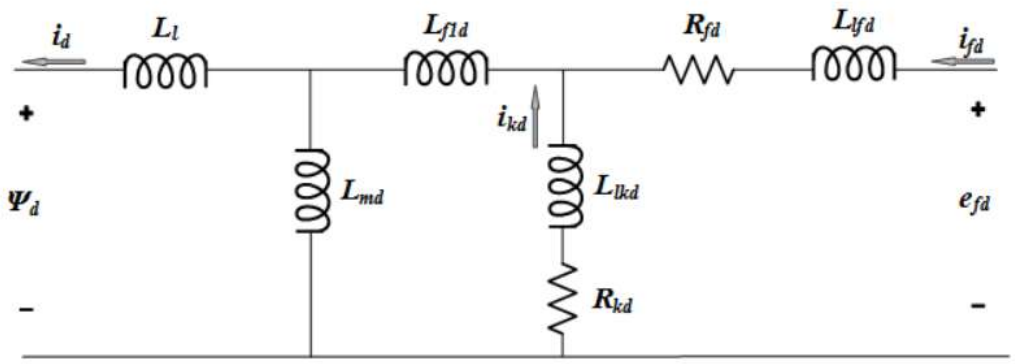

Figure 8 - Per-unit d-axis equivalent circuit. Matlab 2024b.

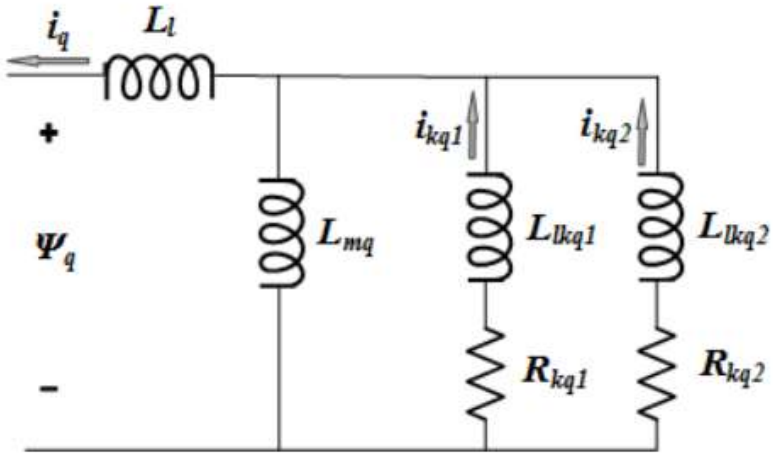

Figure 9 - Per-unit q-axis equivalent circuit. Matlab 2024b.

The equations for analysing a synchronous machine in SIMULINK can be seen in Eq 3 to 11 below.

$$V_d = -i_d R_s - \omega\psi_q + \frac{d\psi_d}{dt} \quad (1)$$

$$V_q = -i_q R_s + \omega\psi_d + \frac{d\psi_q}{dt} \quad (2)$$

$$V_0 = -i_0 R_0 + \frac{d\psi_0}{dt} \quad (3)$$

$$V_{fd} = \frac{d\psi_{fd}}{dt} + R_{fd} i_{fd} \quad (4)$$

$$0 = \frac{d\psi_{kd}}{dt} + R_{kd} i_{kd} \tag{5}$$

$$0 = \frac{d\psi_{kq1}}{dt} + R_{kq1} i_{kq1} \tag{6}$$

$$0 = \frac{d\psi_{kq2}}{dt} + R_{kq2} i_{kq2} \tag{7}$$

$$\begin{bmatrix} \psi_d \\ \psi_{kd} \\ \psi_{fd} \end{bmatrix} = \begin{bmatrix} L_{md} + L_l & L_{md} & L_{md} \\ L_{md} & L_{lkd} + L_{f1d} + L_{md} & L_{f1d} + L_{md} \\ L_{md} & L_{f1d} + L_{md} & L_{lfd} + L_{f1d} + L_{md} \end{bmatrix} \begin{bmatrix} -i_d \\ i_{kd} \\ i_{fd} \end{bmatrix} \tag{8}$$

$$\begin{bmatrix} \psi_q \\ \psi_{kq1} \\ \psi_{kq2} \end{bmatrix} = \begin{bmatrix} L_{mq} + L_l & L_{mq} & L_{mq} \\ L_{mq} & L_{mq} + L_{kq1} & L_{mq} \\ L_{mq} & L_{mq} & L_{mq} + L_{kq2} \end{bmatrix} \begin{bmatrix} -i_q \\ i_{kq} \\ i_{kq2} \end{bmatrix} \tag{9}$$

Where;

V_d is the voltage in the d-axis

V_q is the voltage in the q-axis

V_{fd} is the field voltage in the q-axis

i_d is the rotor current

i_q is the field winding current

ψ is the winding flux linkage

R_s is the rotor resistance

R_f is the field winding resistance

R_k is the damper winding resistance

ω is the rotor electrical angular velocity

L_m is the magnetising inductance

L_l is the leakage inductance

L_{lk} is the damper winding leakage inductance

L_{fl} is the field winding inductance

L_{lf} is the field winding leakage inductance

Simulation using abc-dq for GFMI control

By using the abc to dq0 transformation block (also known as the Park transformation) in SIMULINK, a three-phase (abc) signal can be transformed to a dg rotating reference frame as seen in Figure 10 below.

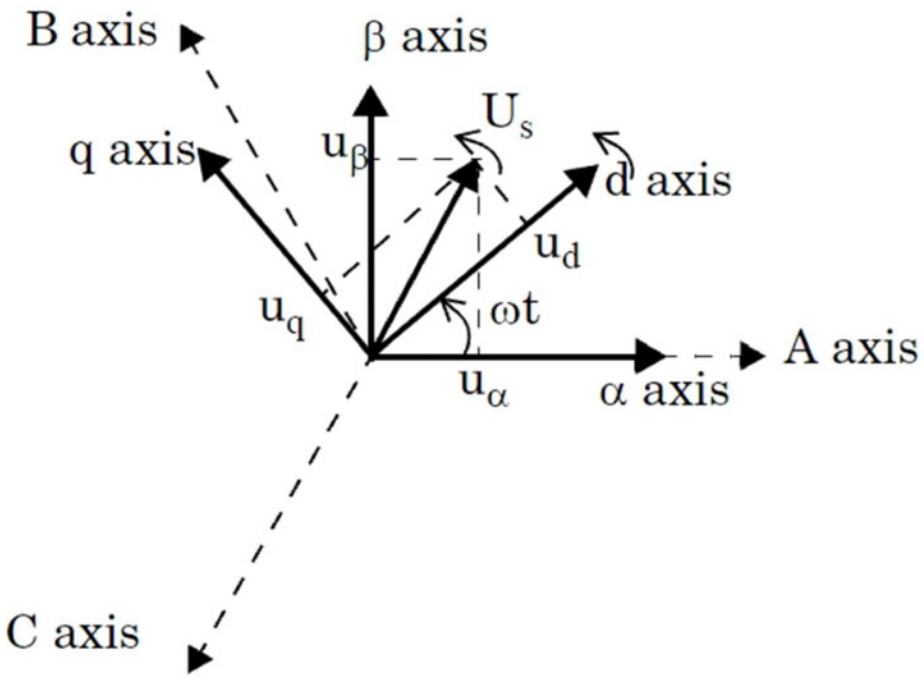

Figure 10 - d, q axis shown in relation to ABC phasor diagram. Matlab 2024a

The values for the d and q-axis can be found from abc values with Equations 10 to 12

$$V_d = \frac{2}{3}\left(V_a\, sin(\omega t) + V_b sin\left(\omega t - \frac{2\pi}{3}\right) + V_c\, sin\left(\omega t + \frac{2\pi}{3}\right)\right) \quad (10)$$

$$V_q = \frac{2}{3}\left(V_a\, cos(\omega t) + V_b cos\left(\omega t - \frac{2\pi}{3}\right) + V_c\, cos\left(\omega t + \frac{2\pi}{3}\right)\right) \quad (11)$$

$$V_0 = \frac{1}{3}(V_a + V_b + V_c) \quad (12)$$

The above equations can also be used in matrix form as per equation 13 below.

$$\begin{bmatrix} V_d \\ V_q \\ V_0 \end{bmatrix} = \frac{2}{3}\begin{bmatrix} cos\,(\omega t) & cos\left(\omega t - \frac{2\pi}{3}\right) & cos\left(\omega t + \frac{2\pi}{3}\right) \\ -sin\,(\omega t) & -sin\left(\omega t - \frac{2\pi}{3}\right) & -sin\left(\omega t + \frac{2\pi}{3}\right) \\ \frac{1}{2} & \frac{1}{2} & \frac{1}{2} \end{bmatrix}\begin{bmatrix} V_a \\ V_b \\ V_c \end{bmatrix} \quad (13)$$

To convert the values from the d and q axis back to abc values, the following Equations 14, 15 and 16 can be used.

$$V_a = V_d\, sin(\omega t) + V_q\, cos(\omega t) + V_0 \quad (14)$$

$$V_b = V_d\, sin\left(\omega t - \frac{2\pi}{3}\right) + V_q\, cos\left(\omega t - \frac{2\pi}{3}\right) + V_0 \quad (15)$$

$$V_c = V_d\, sin\left(\omega t + \frac{2\pi}{3}\right) + V_q\, cos\left(\omega t + \frac{2\pi}{3}\right) + V_0 \quad (16)$$

Again, these equations can be used in matrix form.

$$\begin{bmatrix} V_a \\ V_b \\ V_c \end{bmatrix} = \frac{2}{3}\begin{bmatrix} cos\,(\omega t) & -sin(\omega t) & 1 \\ cos\left(\omega t - \frac{2\pi}{3}\right) & -sin\left(\omega t - \frac{2\pi}{3}\right) & 1 \\ cos\left(\omega t + \frac{2\pi}{3}\right) & -sin\left(\omega t + \frac{2\pi}{3}\right) & 1 \end{bmatrix}\begin{bmatrix} V_d \\ V_q \\ V_0 \end{bmatrix} \quad (17)$$

Proposed GFMI for this research

The proposed GFMI model for this research is based on the paper by Liu, Liu & Zhao (2014). This employs a simple control for GFMI using voltage and current setpoints. Figure 11 below shows the entire control system that employs the abc-dq transform as seen in Liu, Liu and Zhao (2014).

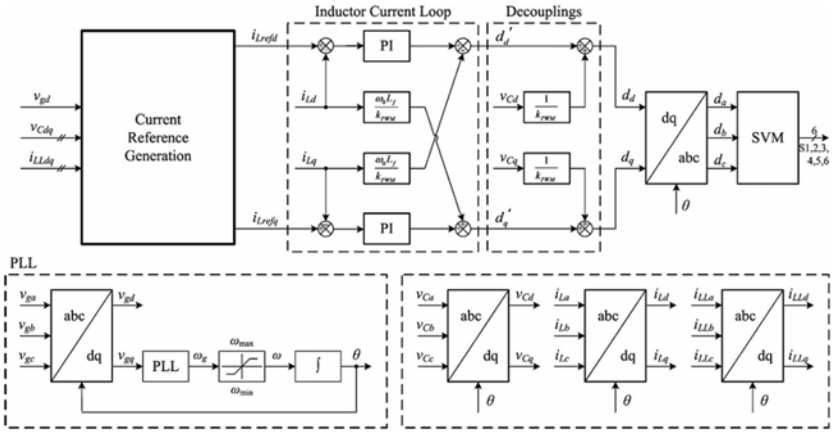

Figure 11 - Overall block diagram of the unified control strategy. Liu, Liu and Zhao 2014.

The simple control system seen in Figure 12 below is the basis for the control system used in the SIMULINK model.

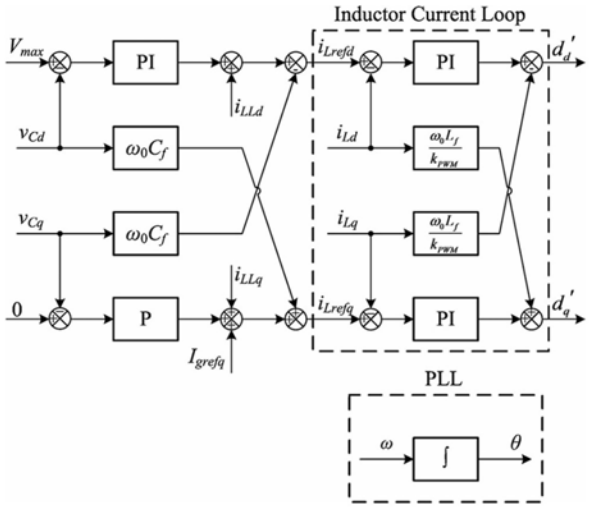

Figure 12 - Simplified block diagram of the unified control strategy when DG operates in Islanded mode. Liu, Liu and Zhao 2014.

The replicated control system in SIMULINK using the previous control strategy can be seen in Figure 13 below.

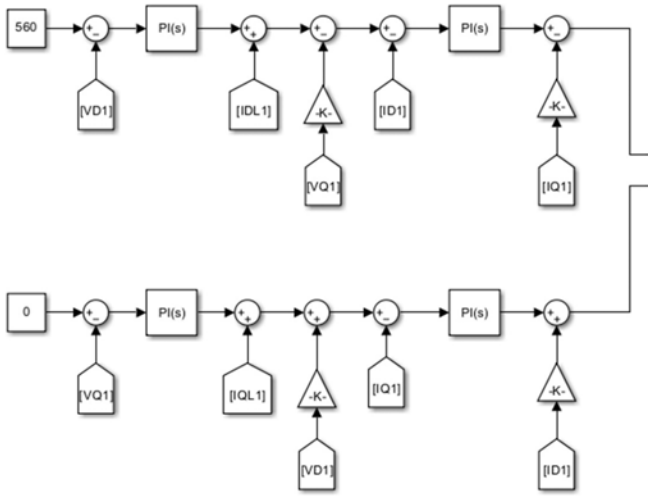

Figure 13 - Control system for GFMI model in SIMULINK

The SIMULINK model uses one inverter as the GFMI, designed for 1MW output, with another three Grid Following Inverter (GFLI)s, designed for 1MW output each, to make a 4MW BESS. The GFLI control system is based on the grid-tied mode from Liu, Liu and Zhao (2014) as seen in Figure 14 below.

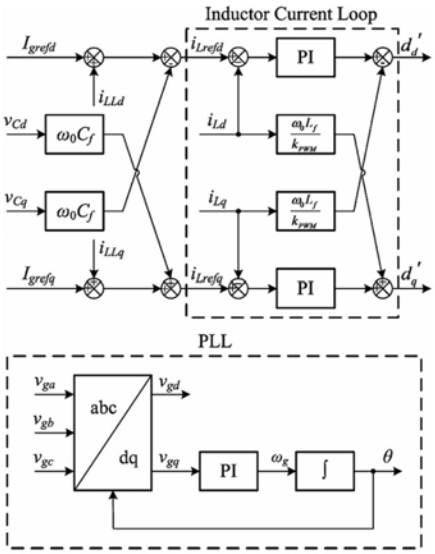

Figure 14 - Simplified block diagram of the unified control strategy when DG operates in the grid-tied mode. Liu, Liu and Zhao 2014.

The control system for the three slave GFLIs uses the d and q-axis currents from the master GFMI for their current setpoint as seen in Figure 15 below.

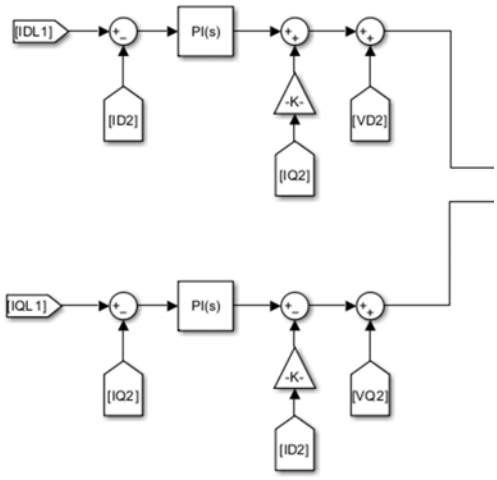

Figure 15 - Control system for GFLI model in SIMULINK

While Liu, Liu and Zhao (2014) discuss switching between control types for grid forming and grid following, the model in this research will only be concerned with providing a restart service.

LCL filter values

As the output of an inverter is controlled by Pulse Width Modulation (PWM), higher-order harmonics are produced. To filter these harmonics an L, LC or LCL filter can be used. As Dursun and Döşoğlu (2019) state, the advantages to using LCL filter on the output of the inverter are that low switching frequencies can be used, the filter is physically smaller than an L or LC filter, there is a lower voltage drop across the filter, and they provide better damping. The LCL filter design used in the GFMI model is seen in Figure 16.

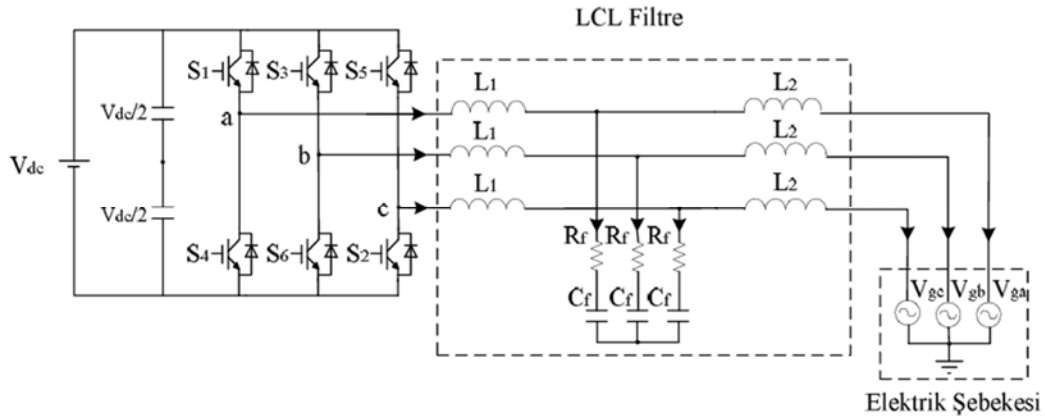

Figure 16 - Voltage source inverter circuit. Dursun and Döşoğlu 2019.

The values used for the LCL filter as shown in Table 1 below. Equations 19 to 30 in Appendix B were used to calculate the parameters of the LCL filter.

Table 1 - LCL filter parameters for 1MW GFMI

System Parameters	LCL Filter Parameters
$V_p = 381V\ (RMS\ Phase\ voltage)$	$L_1 = 38 * 10^{-6}H$
$f_g = 50Hz$	$L_2 = 23 * 10^{-6}H$
$P = 1MW$	$R_f = 0.1\Omega$
$f_{sw} = 10kHz$	$C_f = 183 * 10^{-6}F$

The modelling and simulation will be done in Matlab/Simulink, PowerFactory, and/or PSCAD. In the literature review conducted up to now, all the modelling and simulations were conducted in Matlab/Simulink or PSCAD. Tongge et.al (2020) utilised the IEEE 39 bus system as an example which included 3 PV-BESSs as black start units, 7 generators, 29 loads and 46 transmission lines.

Aurecon (2023) performed their modelling using PSCAD. They developed a simplified but representative and realistic PSCAD model. This simplified model was assumed to be completely disconnected from the rest of the network so that the impact of each modelled element could be observed. The simplified power island model used three technology types:

- Grid-forming BESS
- Synchronous generator
- Grid-following BESS with a synchronous condenser.

In this research, if the initial simulation works, protection systems such as distance, and differential protection will be investigated as to the suitability of creating DRZs. This will involve simulating faults of the modelled network and assessing the response of the DRZ to different faults such as phase to phase, phase to ground and the effectiveness of other protection such as distance protection. The data gathered from these simulations will provide data to support a request to perform live tests.

3.2 Proposed simulation test cases.

While PSCAD is the initial preferred simulation software, it is noted the number of employer-based licenses available to use is limited. To ensure there is no wait time to begin simulations, Simulink will be used to confirm the operation of a grid-forming inverter (GFMI) utilising VSG control.

A simple model of a synchronous generator will be developed to gather base line data on how it responds to known loads. To confirm the Simulink model, a PSCAD (using the free version

of PSCAD) model will also be developed with the same settings and load to confirm the Simulink models.

If the response of the Simulink and PSCAD synchronous generator model corroborate each other, a model of a GFMI can be developed with VSG control in Simulink as the PSCAD free version is limited to 15 nodes.

The Simulink GFMI model will then be tested with the same settings as the Simulink synchronous generator model to compare their response to known loads. If the response of the Simulink synchronous generator and GFMI models corroborate each other, it will be assumed that the GFMI model is operating as a VSG. The GFMI model will then be modified to replicate a known real-world network consisting of 22kV distribution, 66kV sub-transmission, 66/22kV transformers, and 132/66kV transformers.

The data for the transformers will use the standard SIMULINK models which is automatically calculated depending on voltage and transformer rating. The data for the sub-transmission line will be taken from the real-world conductor type, IODINE conductor in this case, and use the MATLAB Line Parameter Calculator to calculate the values for resistance, inductance and capacitance per unit length.

The four proposed test cases will be assessed on system stability and the ability to remain within any statutory limits. A pass or fail will be assigned depending on the model's response to each test case.

3.3 Proposed network layout

The proposed BESS and network layout for the test cases is modelled on a real-world example. Figure 17 shows a schematic of a BESS that is connected to the local distribution network in Central Queensland. It includes 4 inverters with their associated battery banks, a 3 winding transformer, and a circuit breaker (CB) at the PCC.

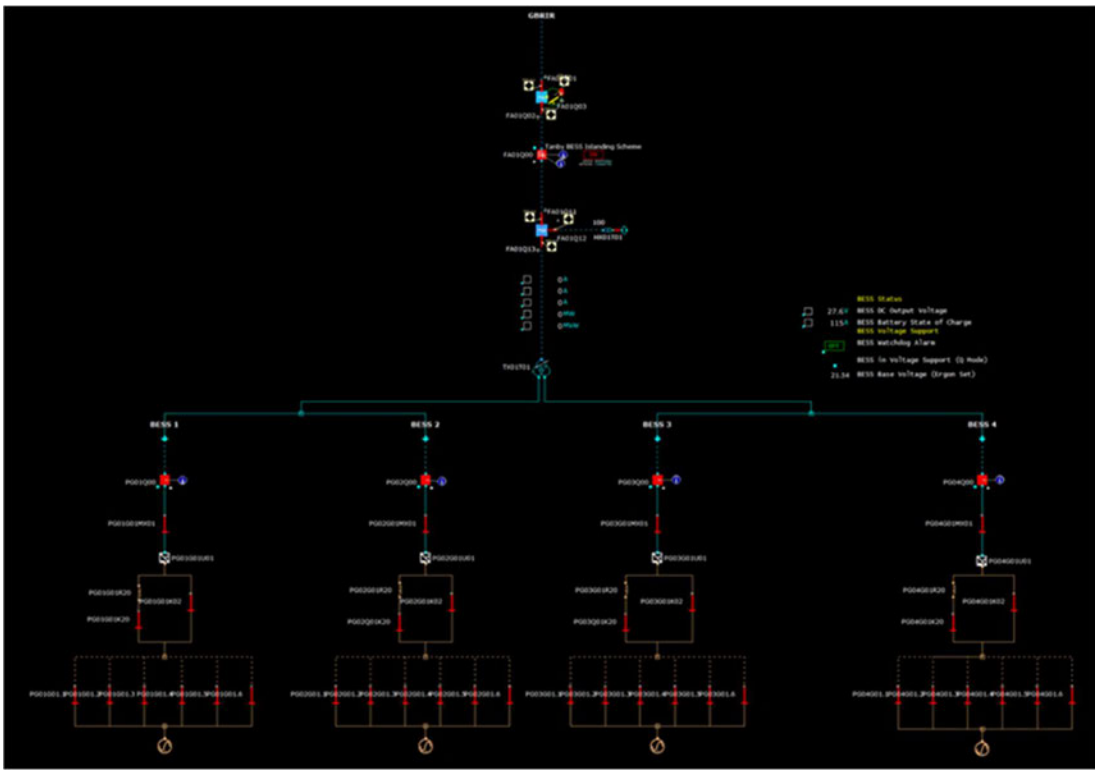

Figure 17 - Proposed BESS layout

Beyond the PCC, it is connected to a substation through a short section of 22kV network. This substation, seen in Figure 18, has a 66/22kV transformer with a 32km section of sub-transmission line connecting it to a second substation, as in Figure 18.

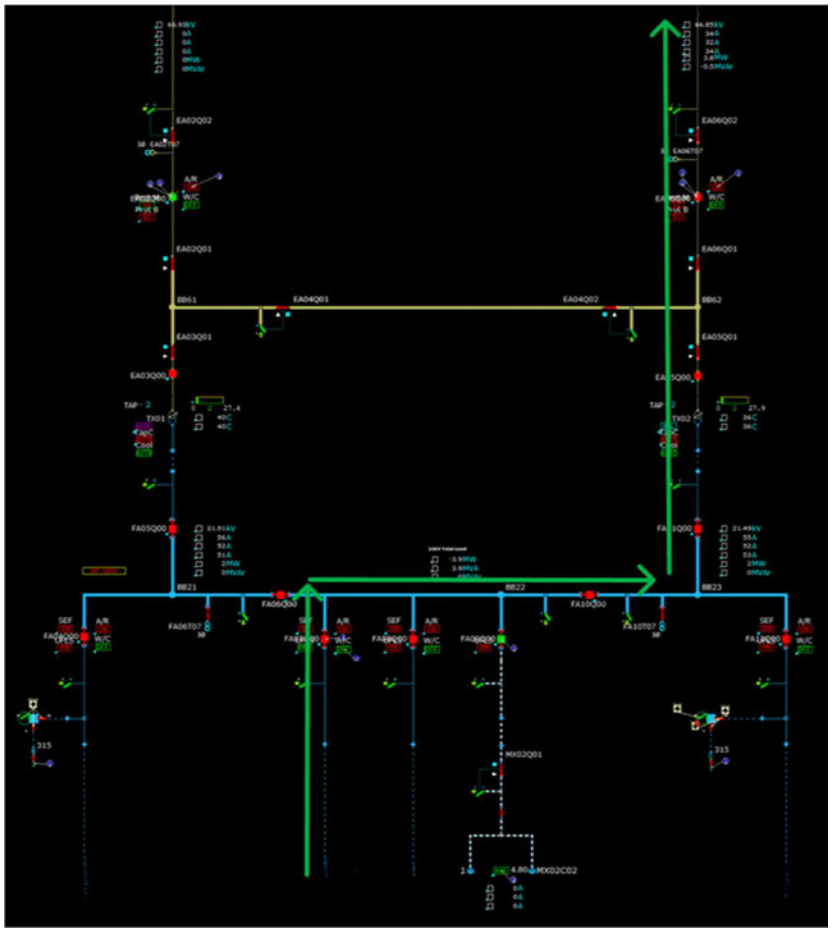

Figure 18 - Substation one layout and path for simulation

The SIMULINK BESS model to be used for simulations is seen in Figure 19. It uses the control strategy from Liu, Liu & Zhao (2014) and mirrors the BESS and network shown in Figures 17 and 18.

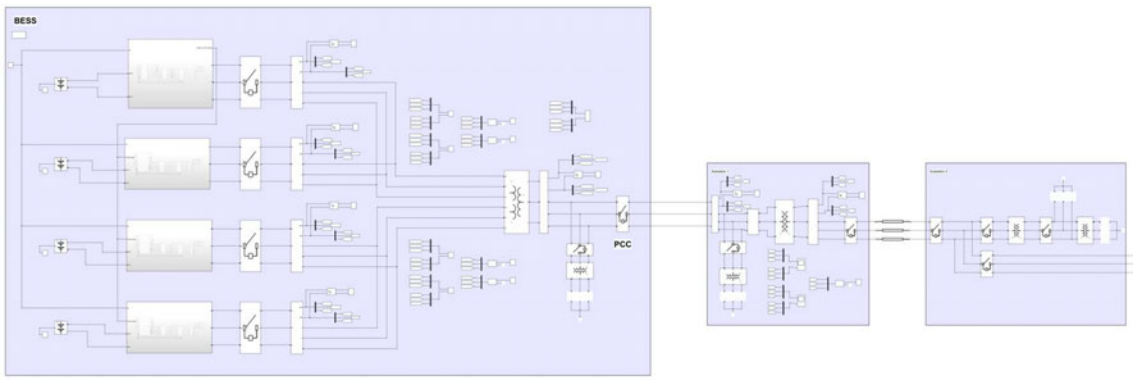

Figure 19 - SIMULINK BESS model

It includes the same equipment as the real-world BESS model with 4 inverters, a 3 winding transformer, and a CB at the PCC. Substation 1 (including a 66/22kV transformer and associated CBs) is connected with a short section of 22kV network. A 32km 66kV sub-transmission line connects Substation 1 to Substation 2.

This model in SIMULINK is designed to be similar to the network for BESS black start live test shown in Figure 20. The black start live tests were performed successfully by National Grid ESO, and following successful simulation in this research, the ability to perform black start live tests with a GFMI BESS will be investigated further. If approved, these live tests would enable the gathering of real-world data to confirm simulated results and provide a basis to develop a Queensland wide DRZ procedure.

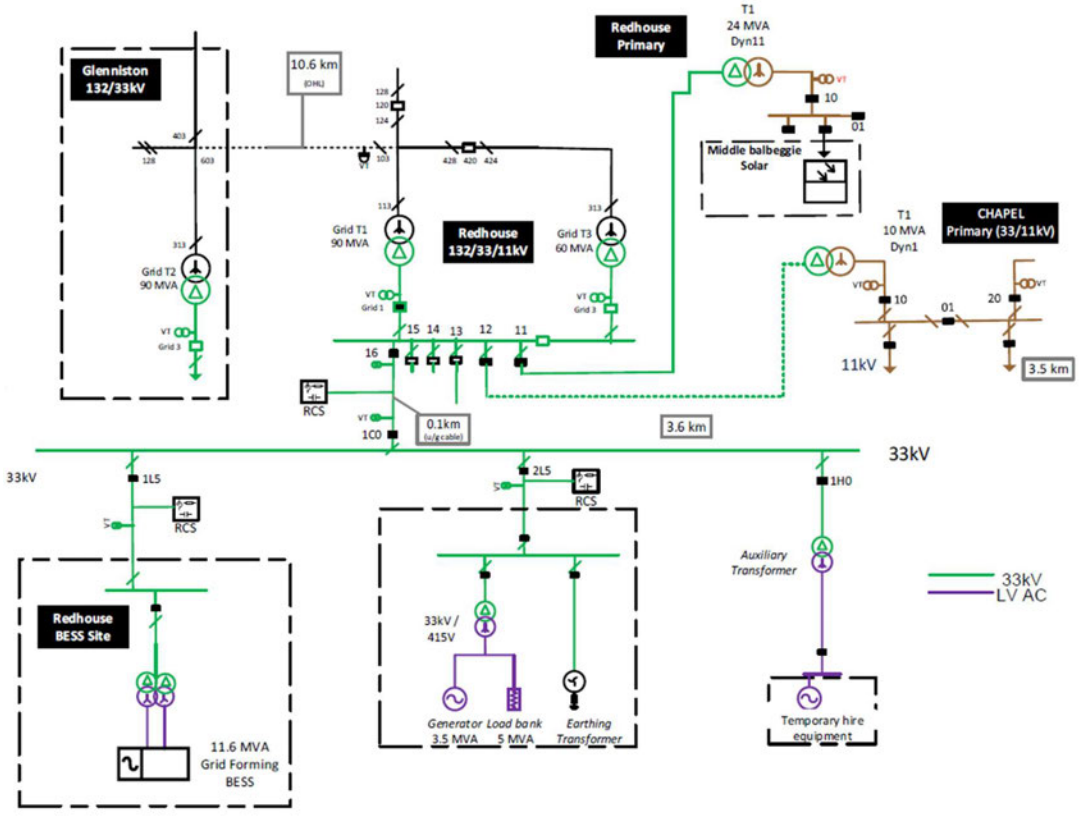

Figure 20 - Network for BESS black start live test (National Grid ESO, 2023a)

CHAPTER 4 RESULTS AND DISCUSSIONS

To confirm the developed model of a GFMI BESS in SIMULINK it was compared to a synchronous generator (SG) model in PSCAD and another in SIMULINK.

4.1Confirmation of SIMULINK GFMI model

Model of synchronous generator in PSCAD

The model in PSCAD to confirm the operation of a GFMI in Simulink uses an Electro-Hydraulic (PID) Governor and AC Exciter controlling a Synchronous Machine (SM). The SMs basic data is shown in Table 2.

Table 2 - PSCAD Synchronous Machine basic data

Setting	**Value**
Rated RMS Line-to-Neutral Voltage	0.23kV
Rated MVA	0.5
Base Angular Frequency	314.159 rad/s

The Base Angular Frequency of 314.159 rad/s is equal to 50Hz.

The SMs output is then connect to a CB that closes at t=0.25 seconds and opens at t=1 seconds. The CB energises a resistive load of 50Ω. This circuit is to see the response of a generator to enable the comparison between PSCAD and SIMULINK. The PSCAD model is shown below in Figure 21.

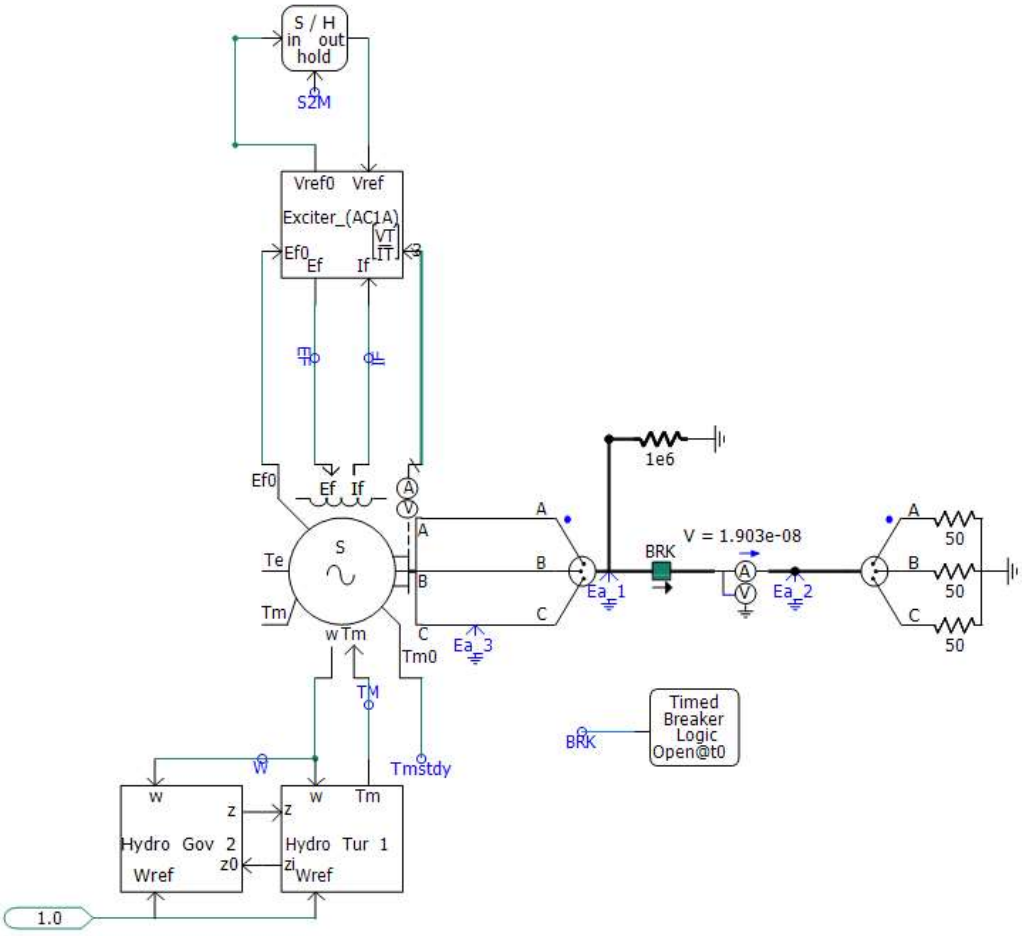

Figure 21 - PSCAD Synchronous Generator model used to confirm SIMULINK GFMI model

When this is simulated over 2 seconds, Figures 22 and 23 show the voltage and current response with load energised at t=0.25 seconds and de-energised at t=1.0 seconds.

The measured values in Figure 22 show 0.5648kV which when calculated using Equation 18 below shows the $V_{L\text{-}Lrms} = 399.4V_{L\text{-}Lrms}$

$$V_{L-L\,RMS} = \frac{V_{L-L\,peak}}{\sqrt{2}} \qquad (18)$$

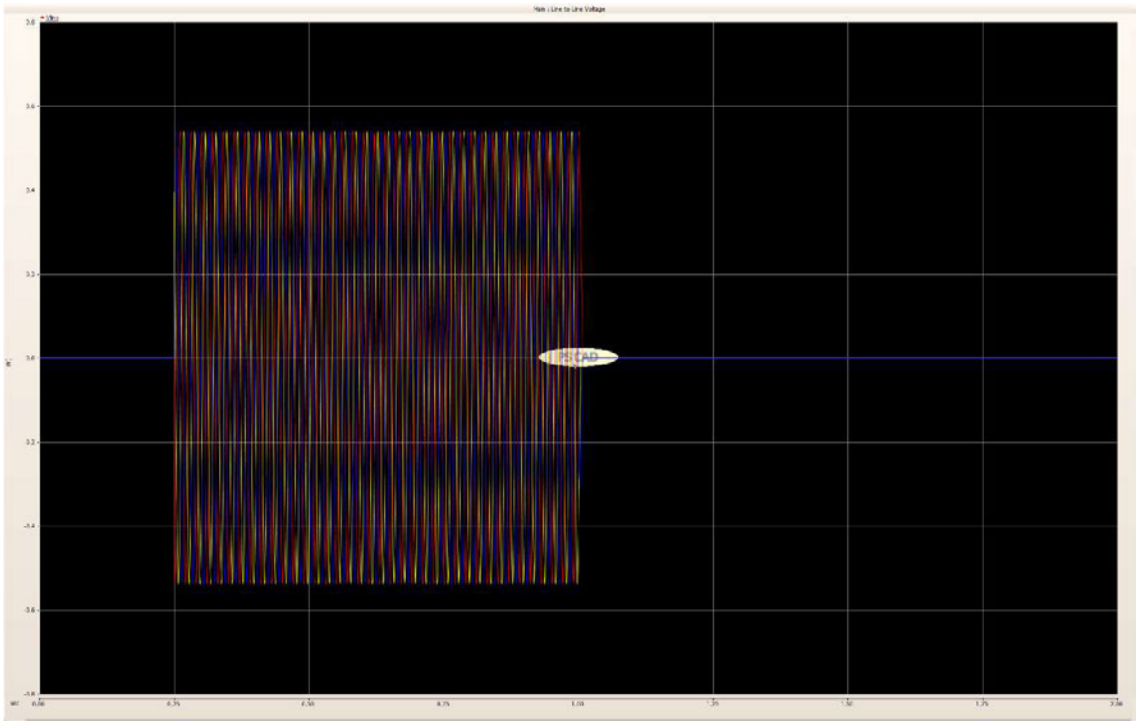

Figure 22 - PSCAD synchronous generator voltage response to resistive load

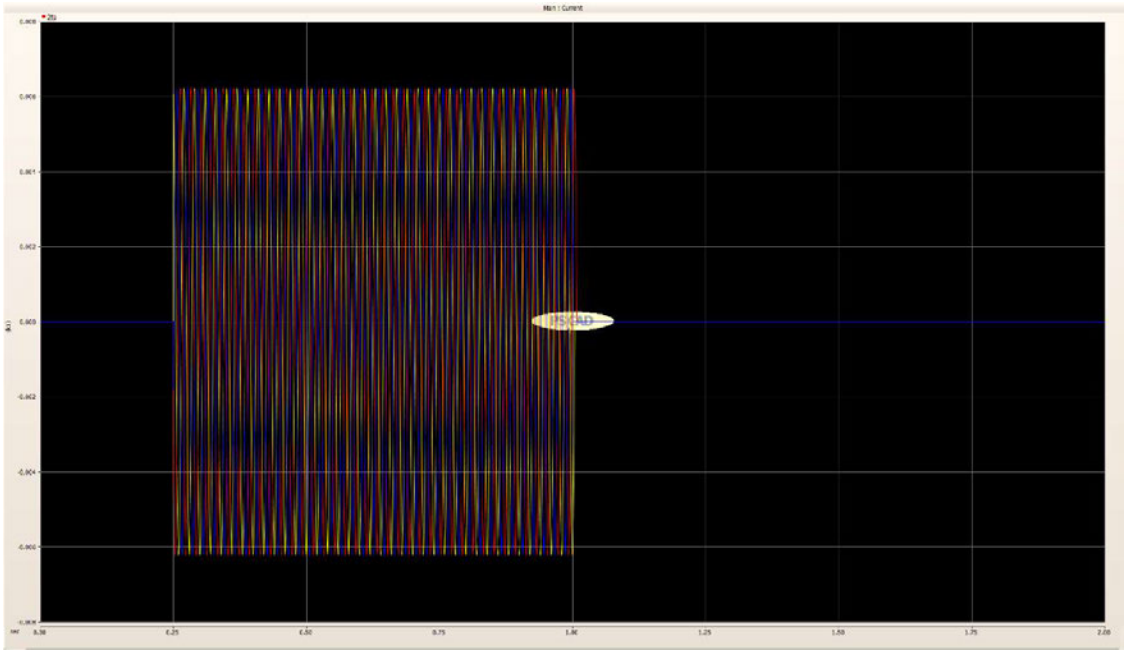

Figure 23 - PSCAD synchronous generator current response to resistive load

Similarly, with Figure 23 showing a peak current of 0.00650kA, the rms current equals $4.59A_{rms}$ per phase. Taking the phase voltage of 230V and the resistive load of 50Ω, the calculated current should be 4.6A. The measured current of 4.59A approximately equals the calculated current of 4.6A.

Model of Synchronous Generator in SIMULINK

The model of the SG in SIMULINK also uses a hydraulic turbine and governor, and an excitation system. The SIMULINK SMs basic data is shown in Table 3 below which corresponds to the PSCAD SM basic data in Table 2.

Table 3 - SIMULINK Synchronous Machine basic data

Setting	**Value**
Line-to-Line Voltage	381 Vrms
Nominal power	5e+5 VA
Frequency	50 Hz

The SIMULINK SG model, shown in Figure 24 below, uses the same layout as the PSCAD SG model. From the terminals of the SM, a CB is used to energise a resistive load with the same values of R=50Ω at t=0.25 seconds and then de-energises at t=1.0 seconds.

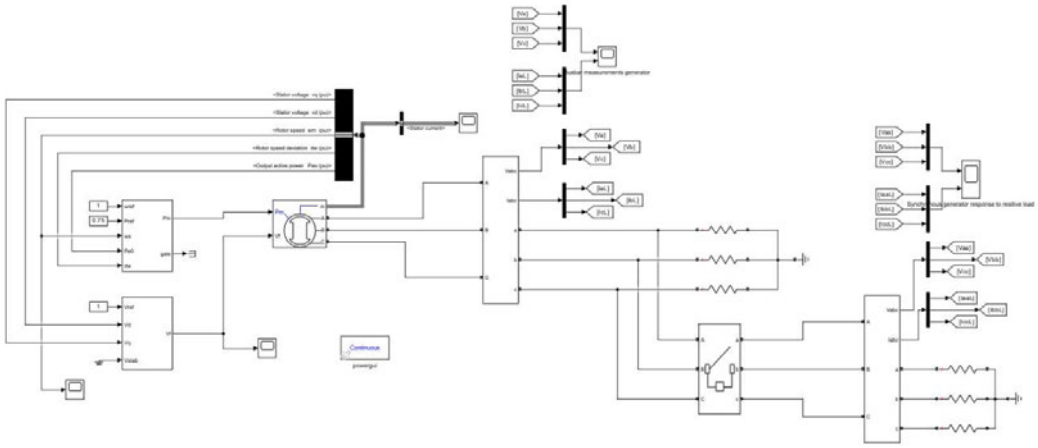

Figure 24 - SIMULINK Synchronous Generator model used to confirm GFMI model

The same test that was conducted with the PSCAD model was simulated for 2 seconds with the CB closing at t=0.25 seconds and opening at t=1.0 seconds. The voltage and current responses are shown in Figure 25.

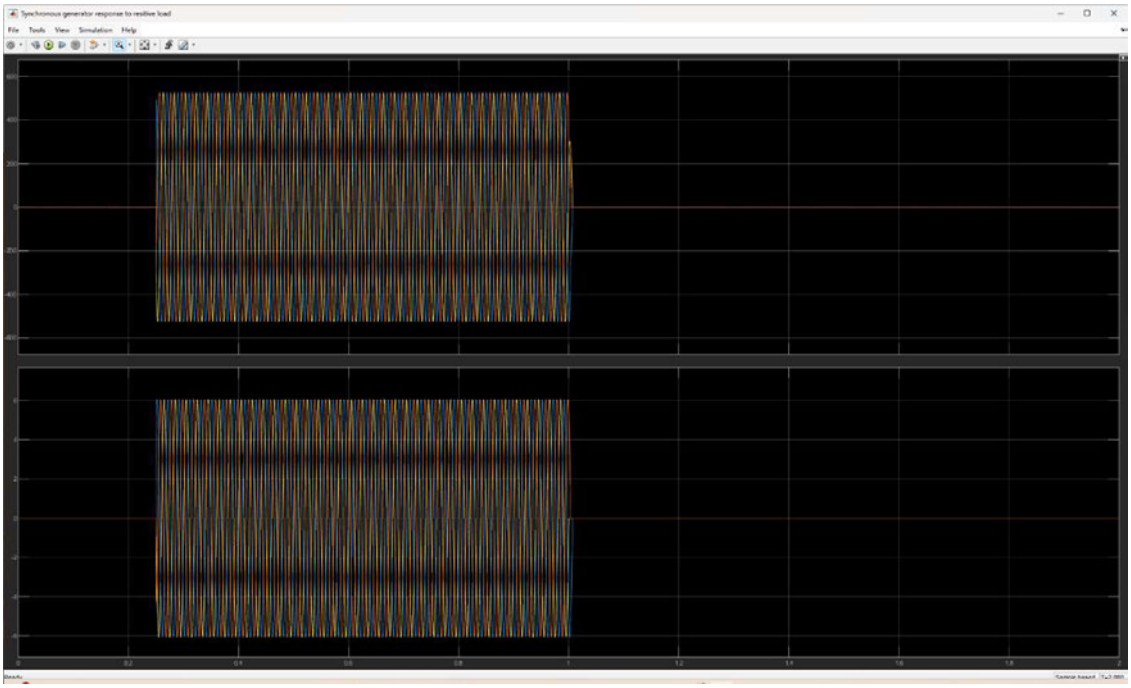

Figure 25 - SIMULINK Synchronous Generator response to resistive load

The values in Figure 25 show the peak line-to-line voltage of $562.4V_{L\text{-}L\ peak}$ when the CB is closed. From these peak values, using Equation 18 above, the RMS values are seen to be $397.68V_{L\text{-}L\ rms}$.

The response of the SIMULINK SG model and the PSCAD SG model is similar, as per Figures 22 and 23, with the voltage showing the set voltage and the current responding as expected to a resistive load.

Model of GFMI BESS in SIMULINK

Using VSG control as the basis of the GFMI with VSG control, the same test circuit used with the synchronous generators can be seen in Figure 26.

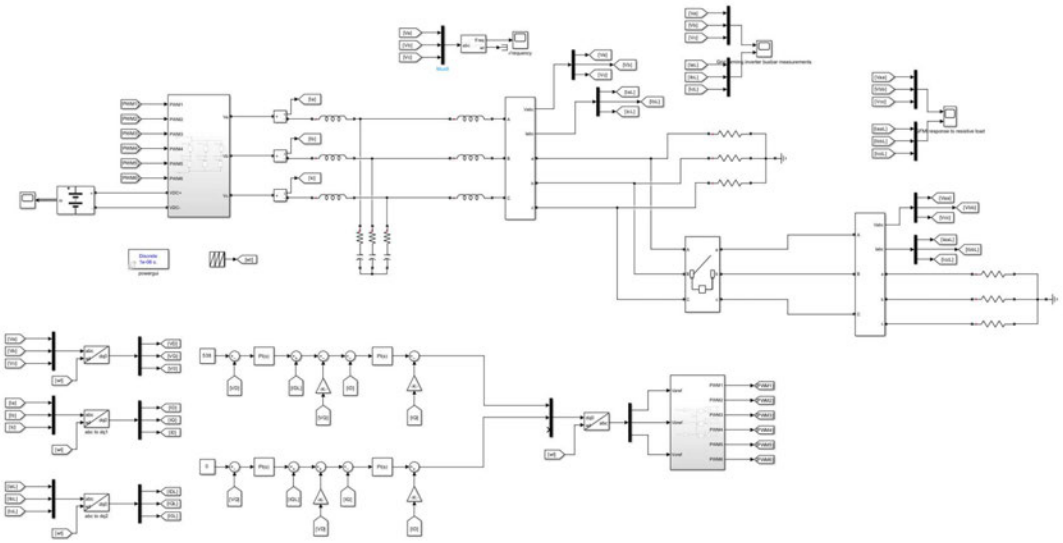

Figure 26 - SIMULINK GFMI model

Synchronous vs Non-synchronous Generation

The response of the GFMI to the same load of 50Ω can be seen in Figure 27. The simulated measured voltage match that of the synchronous generator response as can be seen in Table 4.

Table 4 - Test results for simulation models

Model	**Voltage setpoint ($V_{rms\ phase}$)**	**Measured voltage ($V_{rms\ phase}$)**
Synchronous Generator PSCAD	230	230.6
Synchronous Generator SIMULINK	230	229.4
Virtual Synchronous Generator SIMULINK	230	229.4

Figure 27 shows the voltage (top) and current (bottom) waveforms of the SIMULINK GFMIs response to the same conditions as the synchronous generator models.

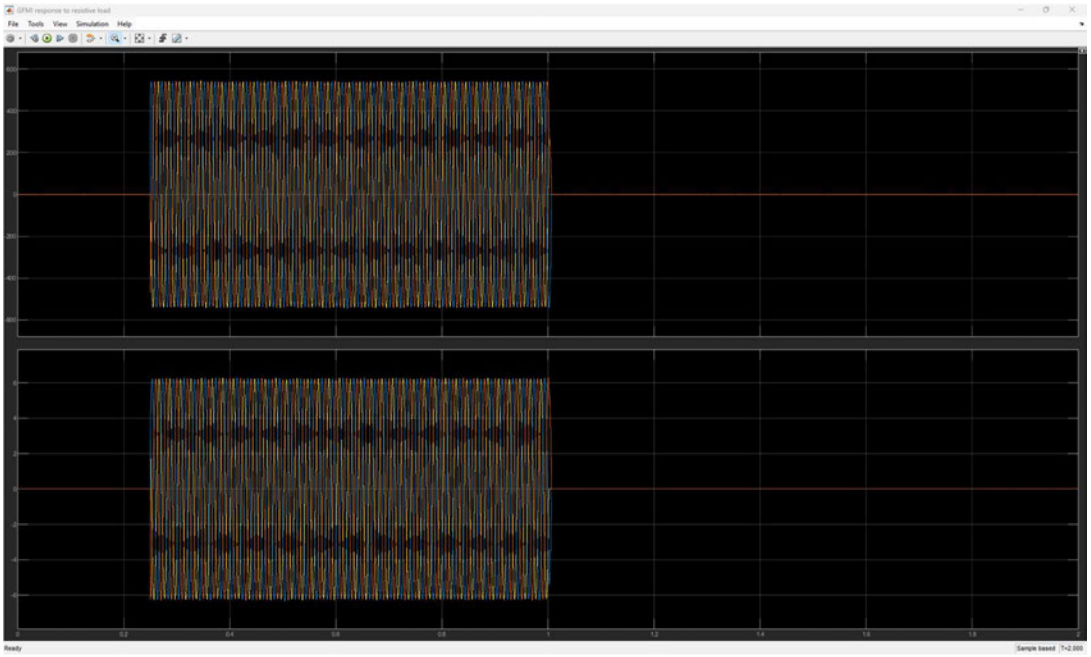

Figure 27 - SIMULINK GFMI model response to resistive load

Figure 28 shows the voltage and current waveforms of the GFMI when zoomed in. The voltage and current values shown in Figure 28 correspond to those already seen in Figures 22, 23 and 25 above.

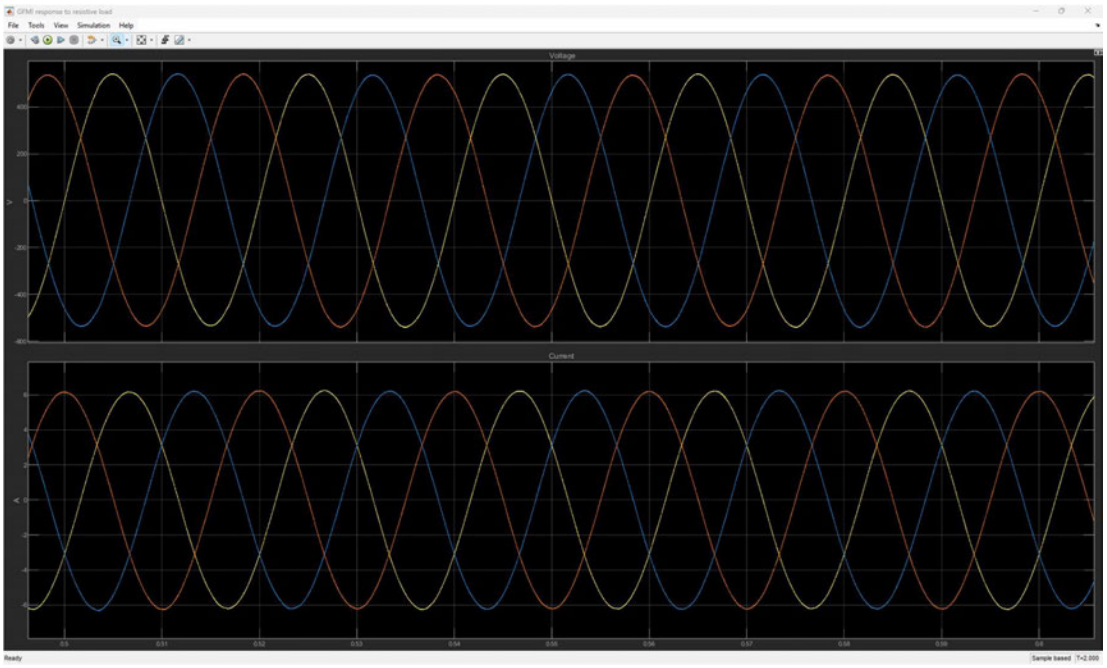

Figure 28 - Zoomed GFMI voltage and current response

4.2 Test Case 1

The model of a 4MW/8MWH GFMI BESS used for the test cases can be seen in Figure 29.

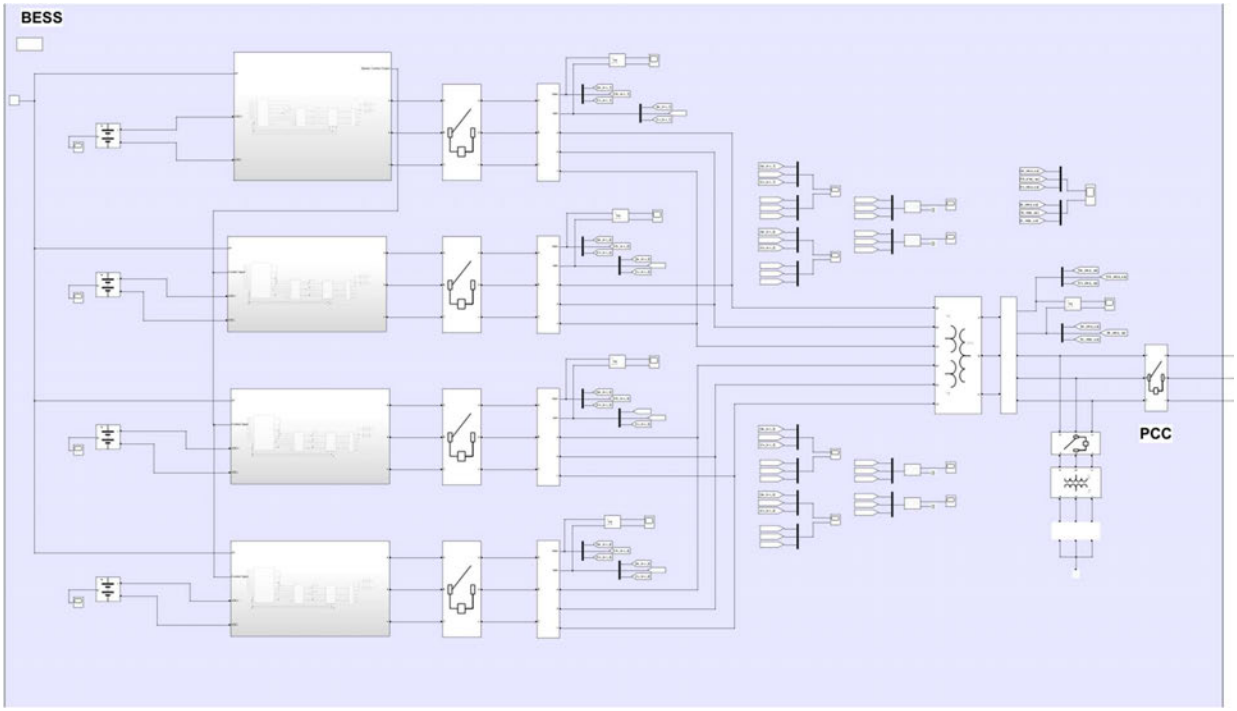

Figure 29 - BESS model for system re-start

When energised up to the PCC, all four inverters share the load evenly. There is approximately 200kW of self-consumption due to station services such as active battery cooling and system monitoring.

Figure 30 below shows the voltage and current waveforms of inverter 1 with all inverters energised up to the PCC. The voltage and current response of the other inverters can be seen in Appendix A.

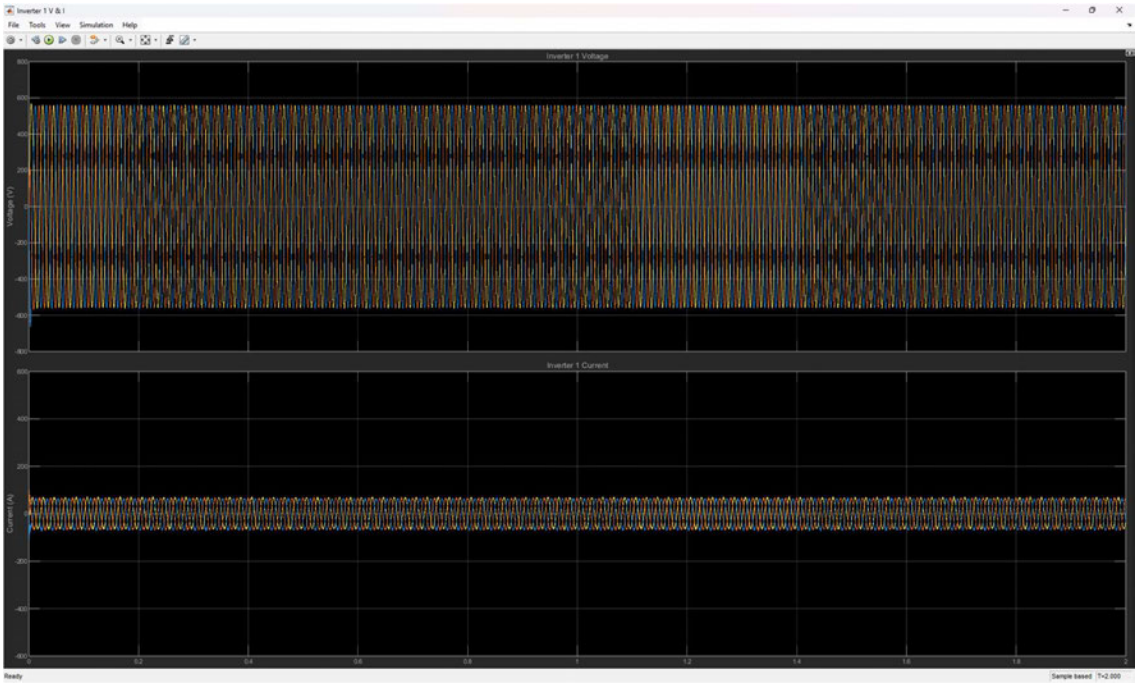

Figure 30 - Inverter 1 Voltage and Current

Figure 31 shows a zoomed in version of Figure 23 at t=0.8 seconds to t=1.2 seconds.

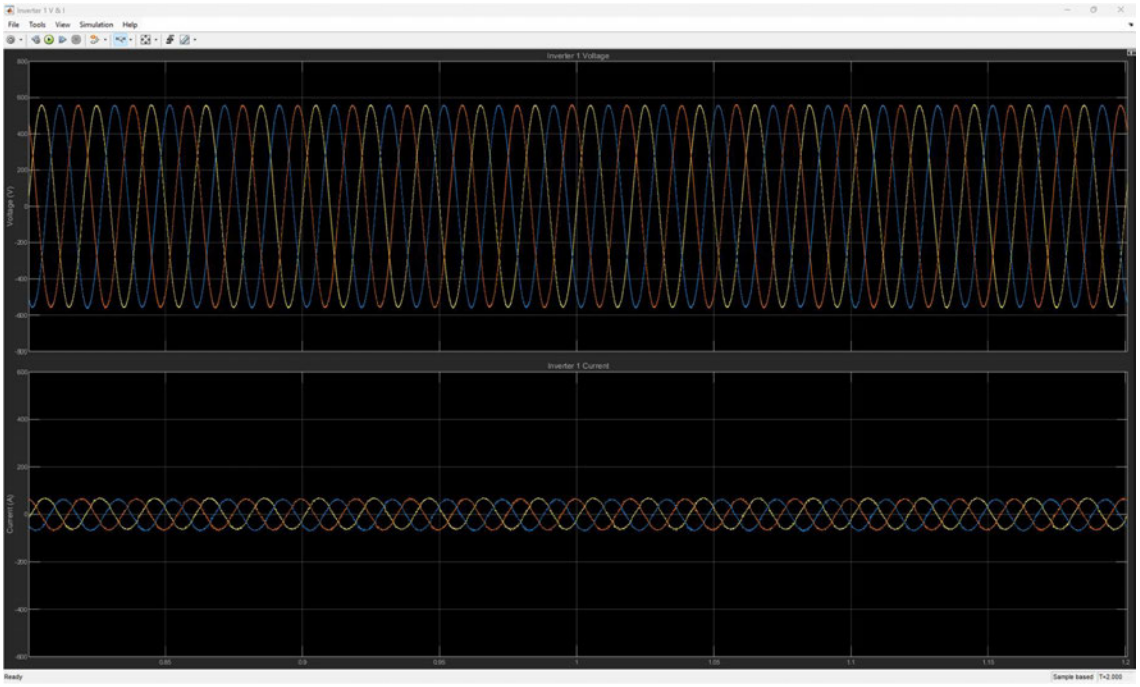

Figure 31 - Inverter 1 Voltage and Current between t=0.8 seconds and t=1.2 seconds

The power supplied by Inverter 1 in Figure 32 shows the power self-consumption of the BESS. This is for monitoring systems and active cooling for the battery packs in a real-world situation. The power supplied by the other inverters was similar with their plots shown in Appendix A.

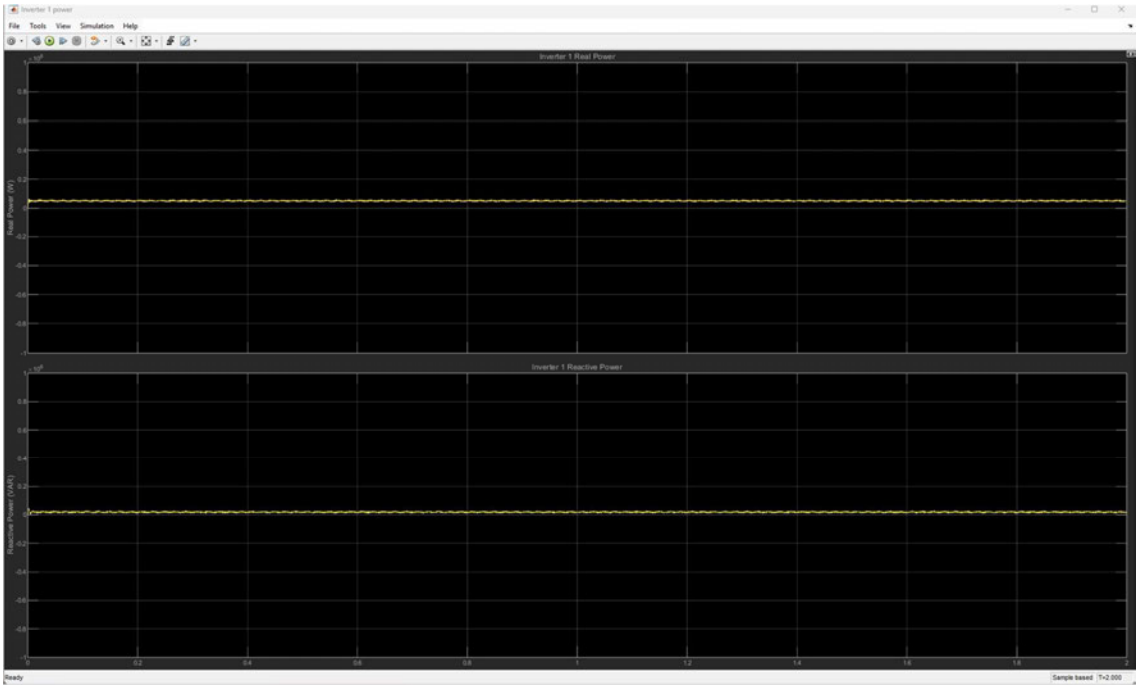

Figure 32 - Inverter 1 Power. Scaled to full power output

The voltage and current values were measured on the high voltage side of the three-winding transformer as shown in figure 33 below. The measured voltage showed a peak of 26.88kV before settling at 22kV. The measured current of 6.39A means that when calculated, there is a self-consumption load of 140kW on site. The peak of 26.88kV is within the allowable overvoltage for a 22kV system.

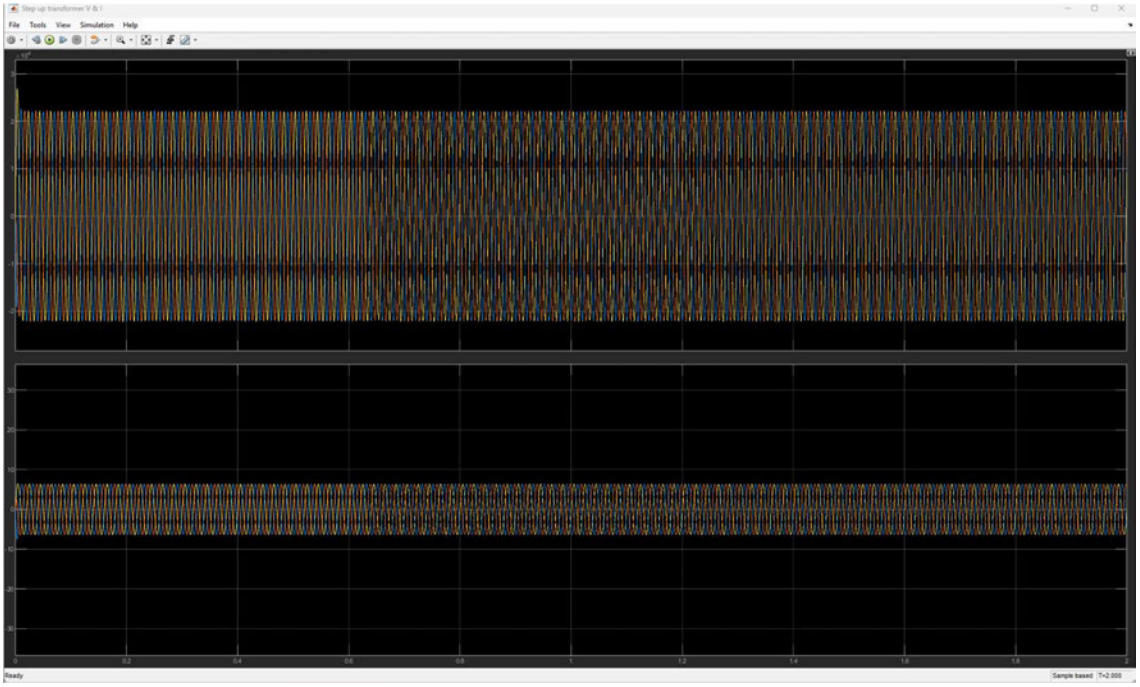

Figure 33 - Step-up transformer

Figure 34 below shows a zoomed in version of Figure 33 at t=0.8 seconds to t=1.2 seconds.

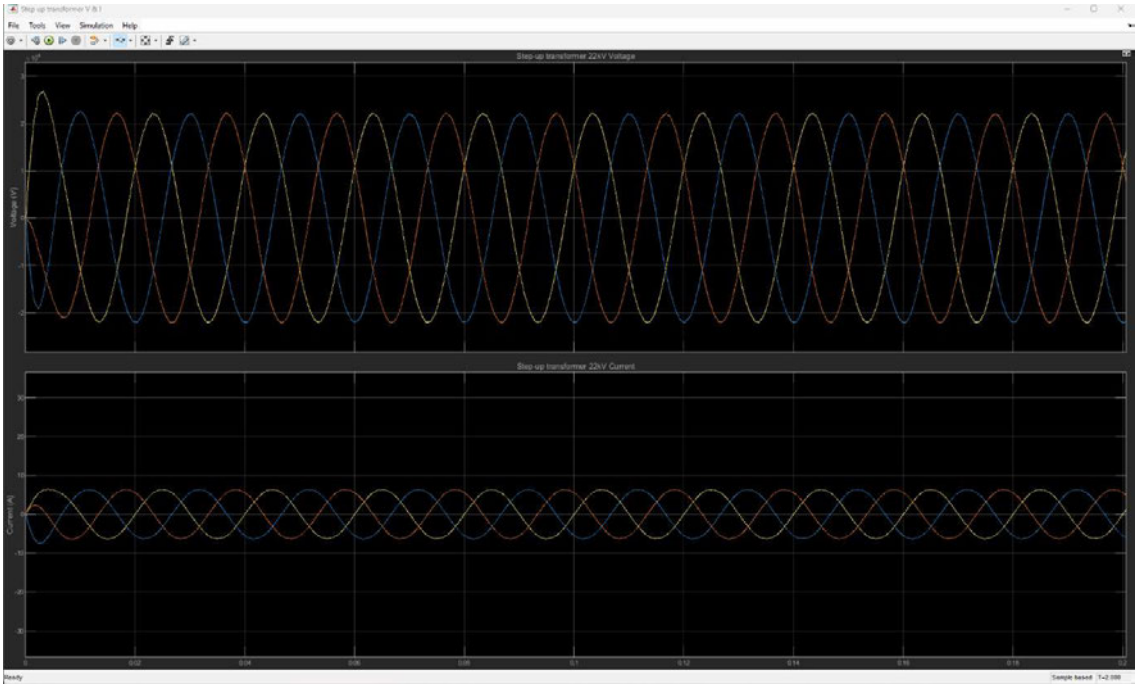

Figure 34 - Step-up transformer from t=0 seconds to t=0.2 seconds

Figure 35 below shows the system power on the HV side of the three-winding transformer. A zoomed version of Figure 35 is shown in Figure 36 between t=0 seconds to t=0.2 seconds. It shows that on energisation at t=0 seconds, the peak real power to energise the three-winding transformer and a 200kW load is 257kW and 158.8kVAR giving a total of 302kVA. This then settles to 186.7kW and 107.8kVAR which gives a steady load or 215kVA. For the purpose of this modelling the self-consumption load is assumed to be mainly resistive.

Figure 35 - Step-up transformer power. Scaled to full power output.

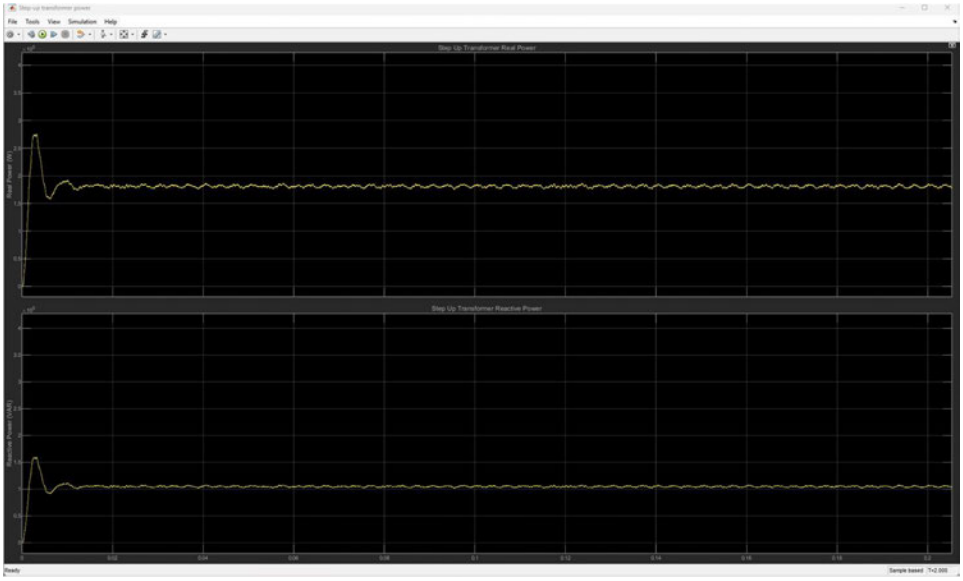

Figure 36 - Step-up transformer from t=0 seconds to t= 0.2 seconds

The frequency response of Inverter 1 is shown in Figure 37 below. The normal operating limits as specified by AEMO are 50Hz ± 0.15. The frequency can be seen to stay within the statutory limits at the 50Hz setpoint for the entire test. Test Case 1 is a pass.

The frequency response of the other inverters can be seen in Appendix A.

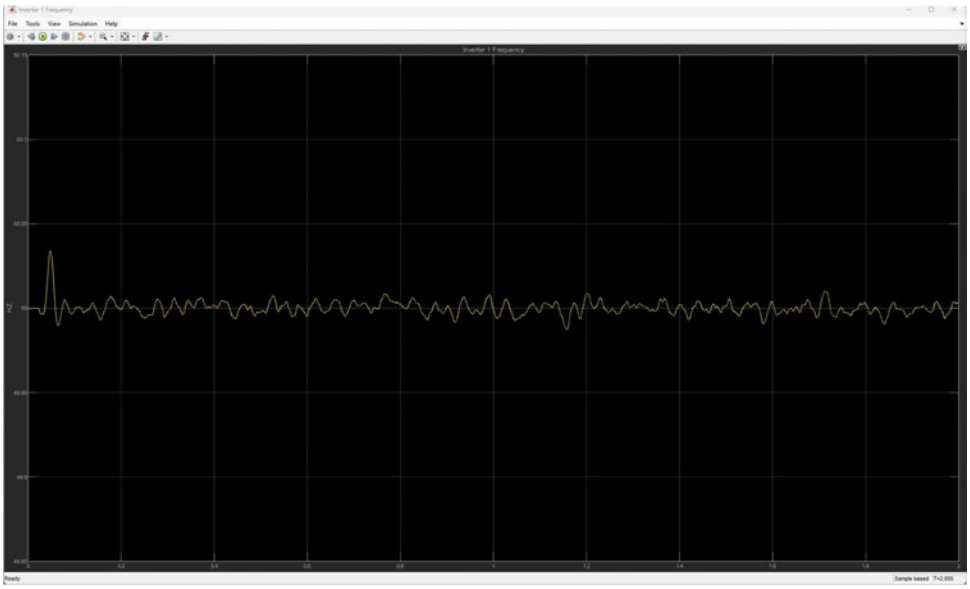

Figure 37 - Inverter 1 frequency response

4.3 Test Case 2

This test built on Test Case 1 with Substation 1, seen in Figure 38, energised. The 22kV PCC CB is closed at 1 second energising the 66/22kV transformer at Substation 1 from the 22kV side.

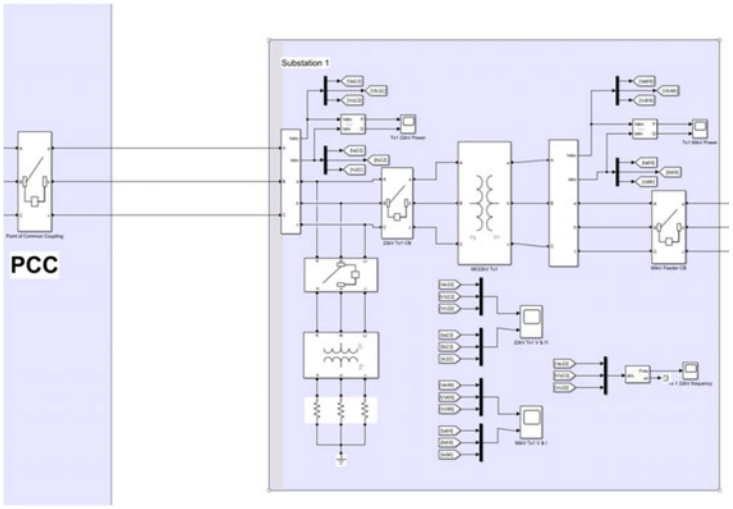

Figure 38 - Test case 2 schematic

The voltage and current response of the CB closing at t=1 seconds is shown in Figure 38.

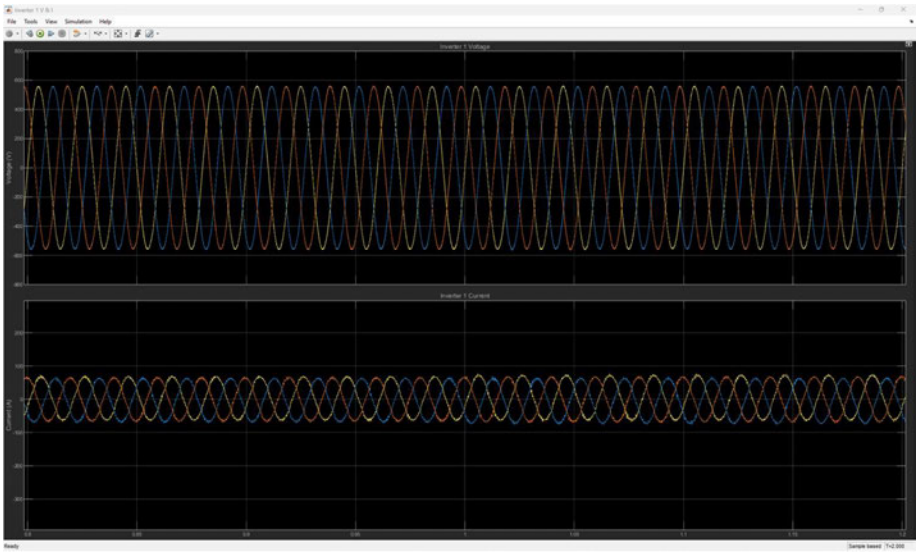

Figure 39 - Inverter 1 Voltage and Current at t=1 seconds energising Transformer 1

All other inverters responded similarly with an increase in current on each phase of approximately 10A. At the inverters there were no noticeable voltage or current transients energising the 66/22kV Transformer 1.

The inverter power output also saw a similar increase at t=1 seconds as shown in Figure 40. Before the CB is closed at t=1 seconds a fluctuation in the power can be seen. After the CB is closed and the 66/22kV transformer is energised a more pronounced power fluctuation can be seen at the inverter output.

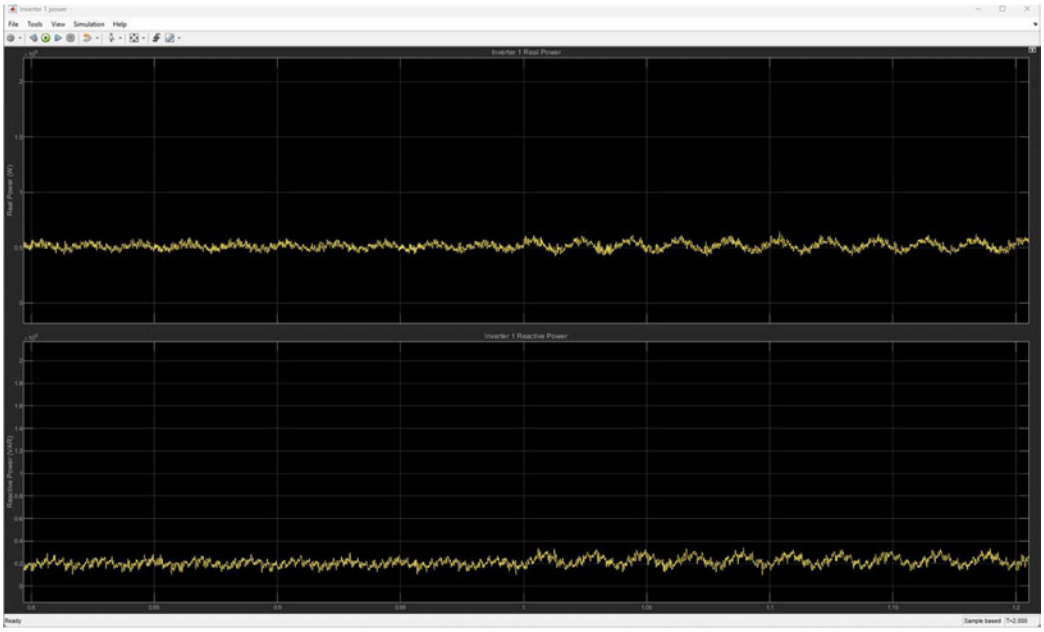

Figure 40 - Inverter 1 Real and Reactive Power at t=1 seconds

From the values in Figure 40 above, the real power supplied by Inverter 1 increased from 57kW before Transformer 1 was energised to 60.26kW following energisation. Reactive power increased from 17.94kVAR to 22.87kVAR which gives an increase from 59.76kVA to 64kVA. All inverters had similar increases.

The power at the 22kV side of Transformer 1 is seen in Figure 41 below. The power fluctuations that were seen at the inverter outputs appears more pronounced on the 22kV side of the 66/22kV transformer after energisation.

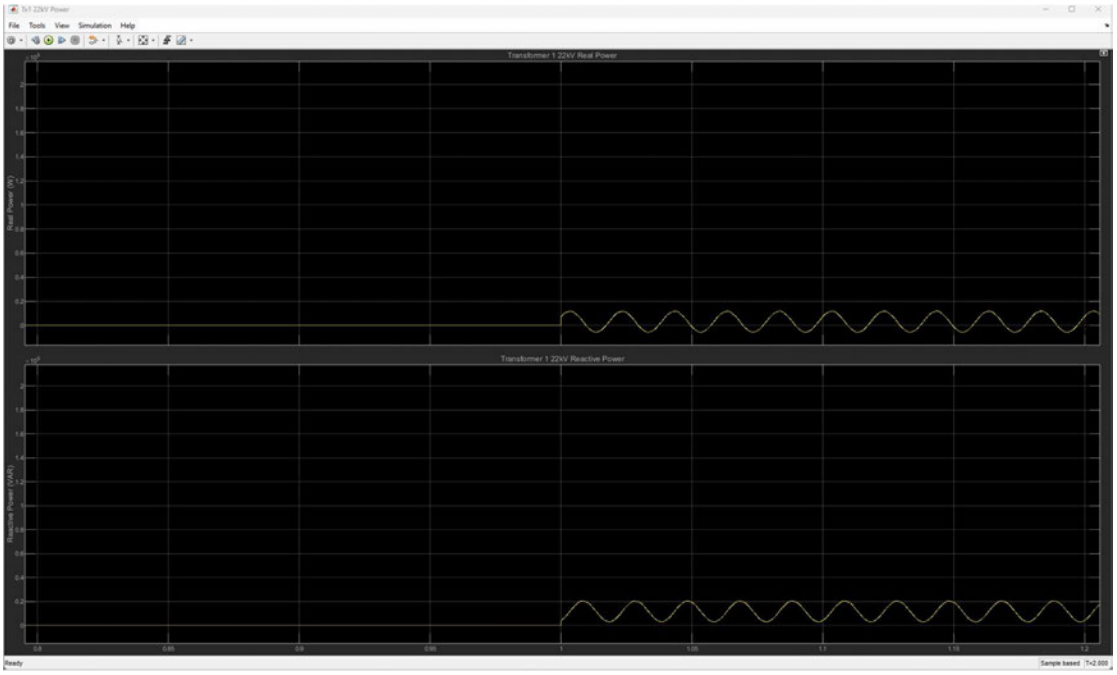

Figure 41 - Transformer 1 22kV Real and Reactive Power after energisation at t=1 seconds

The frequency response of Inverter 1 shown in Figure 42 below shows no adverse change when energising Transformer 1 at t=1 seconds. The frequency remains well within the required statutory limits. Test Case 2 is a pass.

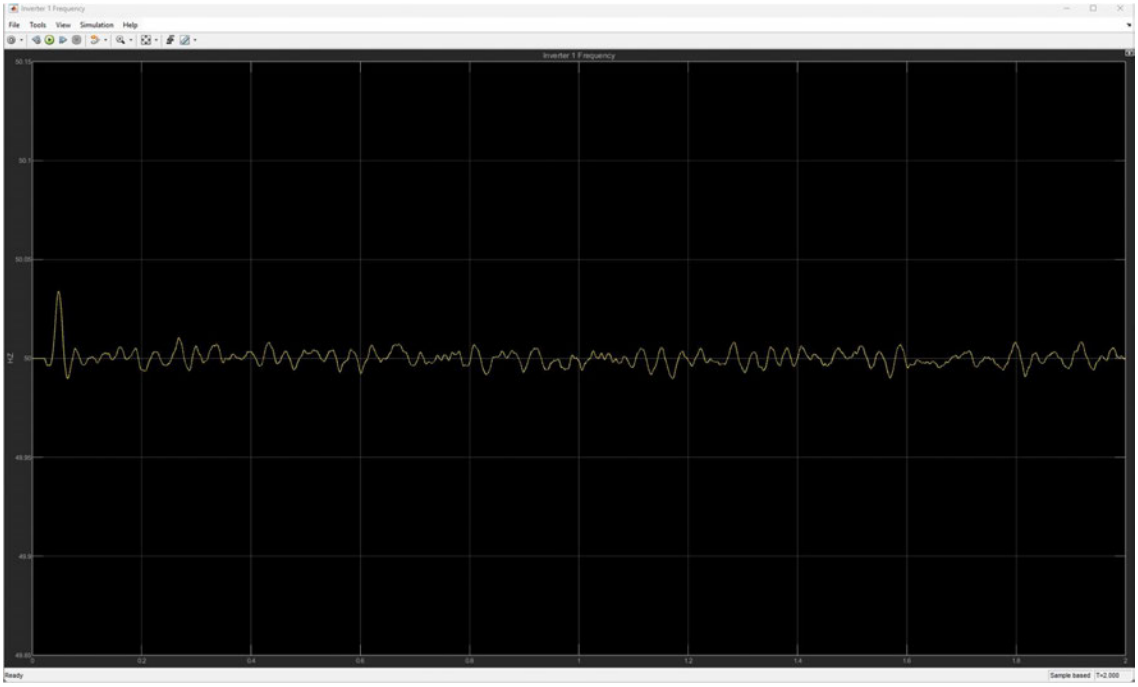

Figure 42 - Inverter 1 frequency response

4.4 Test Case 3

This test case builds on the previous two test cases. The 32km 66kV sub-transmission line, shown in Figure 43, is energised at t=1 seconds after Substation 1 is energised at t=0.5 seconds.

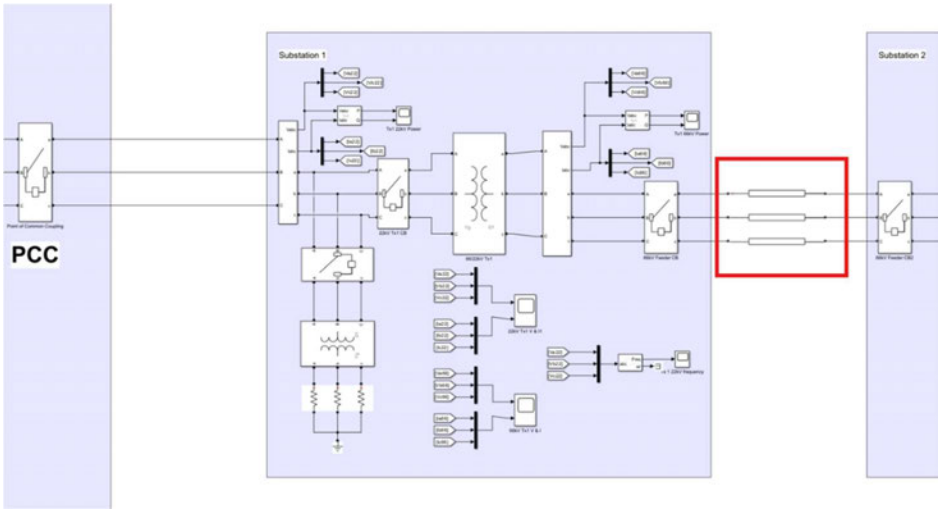

Figure 43 - Test Case 3 schematic

The voltage and current response is seen in Figure 44.

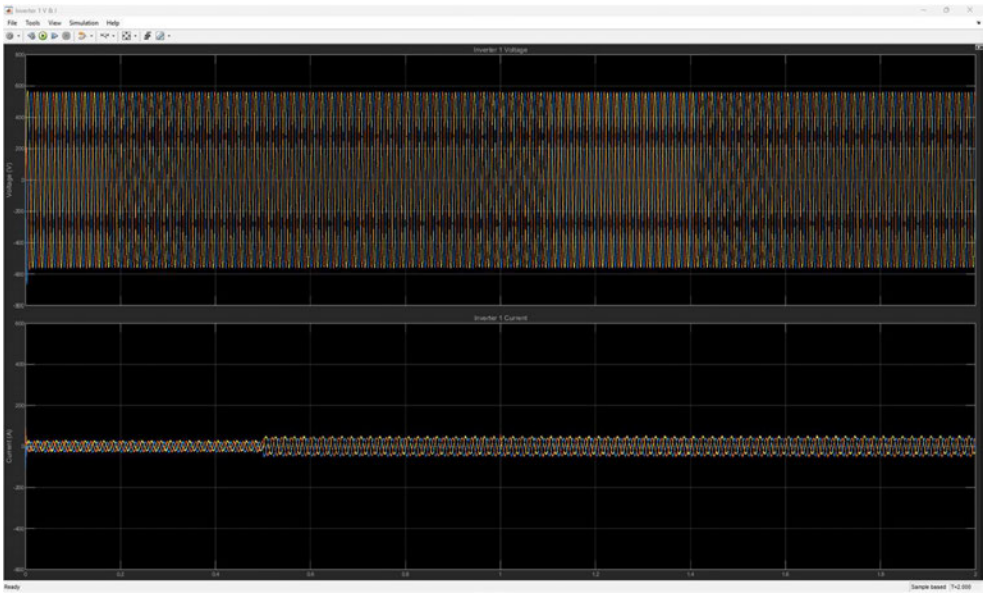

Figure 44 - Inverter 1 response to Test Case 3

Figure 45 shows the response to Test Case 3 when zoomed in between t=0.4 seconds and t=1 seconds.

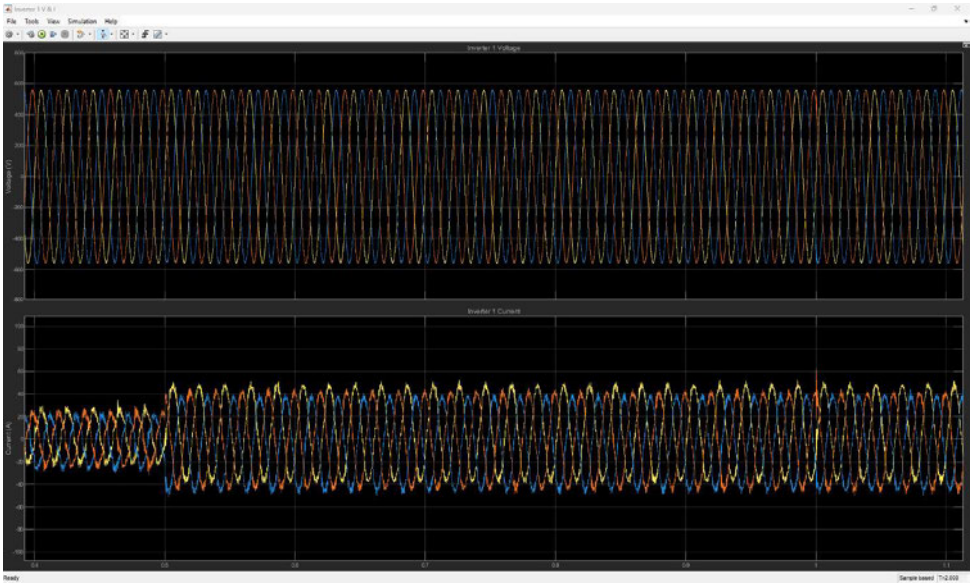

Figure 45 - Inverter 1 response to Test Case 3 between t=0.4 seconds to t=1.1 seconds

When the 32km sub-transmission line is energised at t=1.0 seconds a current transient of approximately 20A can be seen. This will not present any major issues.

Figure 46 below shows the voltage and current transient of Inverter 1 at t=1.0 seconds. The noisy current waveform was investigated but no cause could be found.

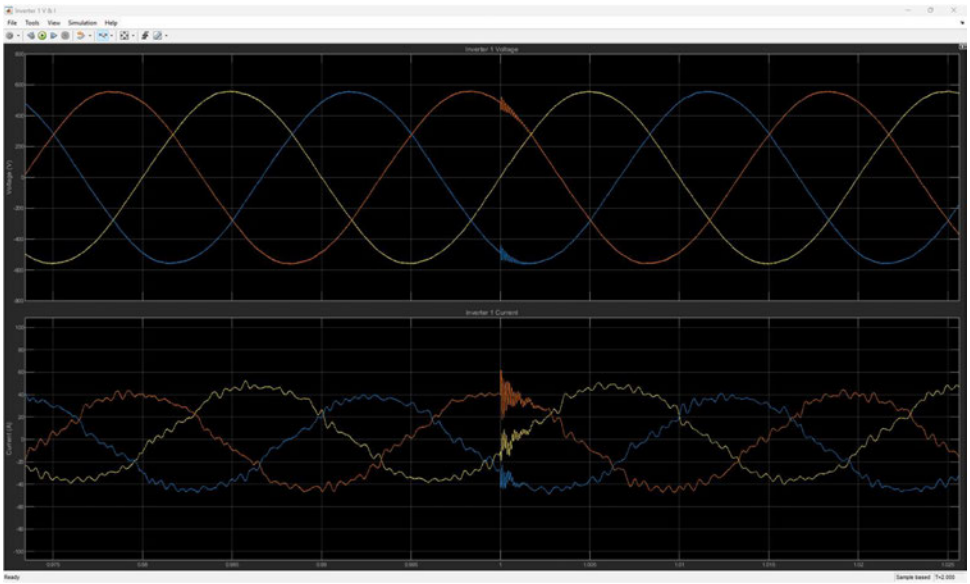

Figure 46 - Inverter 1 Voltage and Current transients at t=1.0 seconds

All other inverters saw the same voltage and current transient when energising the sub-transmission line.

Looking at the 22kV voltage and current waveforms, the transient can be seen clearly at t=1.0 second in Figure 47. While there is no issue with the current transient, the blue phase voltage shows a temporary overvoltage (TOV) of 30kV. This requires further investigation and due to the TOV of 30kV on a 22kV system, this test case is a fail.

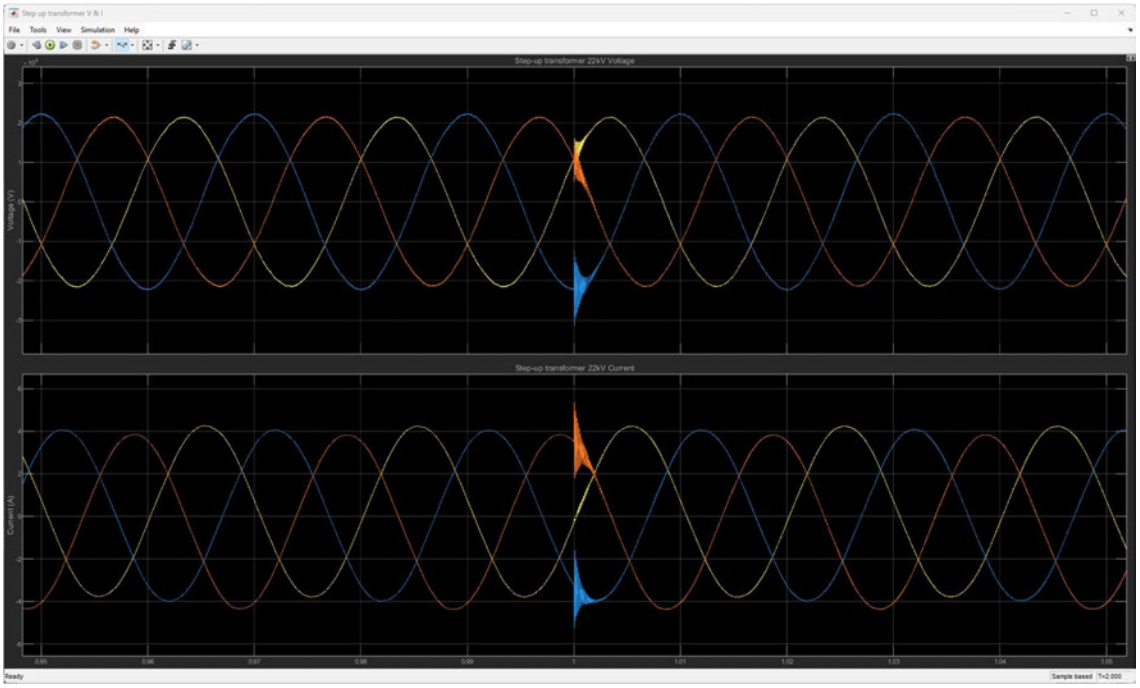

Figure 47 – Step-up Transformer 22kV Voltage and Current

4.5 Test Case 4

While Test Case 3 was a fail, to see what effect energising a second substation with resistive load had, Test Case 4 was run. The SIMULINK model layout is seen below in Figure 54. This test case energised the second substation at t=1.5 seconds after everything else was energised.

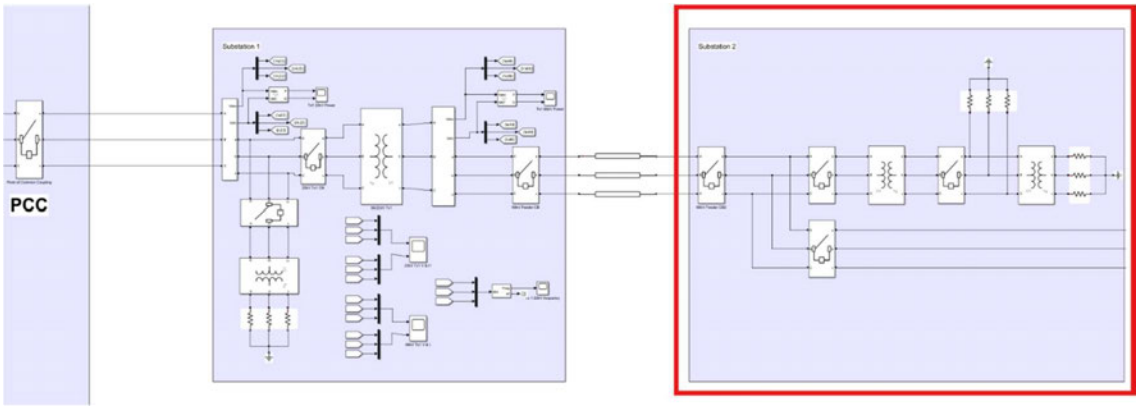

Figure 48 - Test Case 4 schematic

The voltage and current waveform of Inverter 1 in Figure 55 shows the same response as the other test cases until substation 2 is energised at t=1.5 seconds. The voltage waveform remains at the set point, but the current waveform starts drifting away from the zero point, almost as if a DC offset is being introduced. Investigation into why this was happening failed to identify a cause. If a DC offset is being introduced, in a real situation this could cause saturation of transformer cores and cause protection to operate incorrectly.

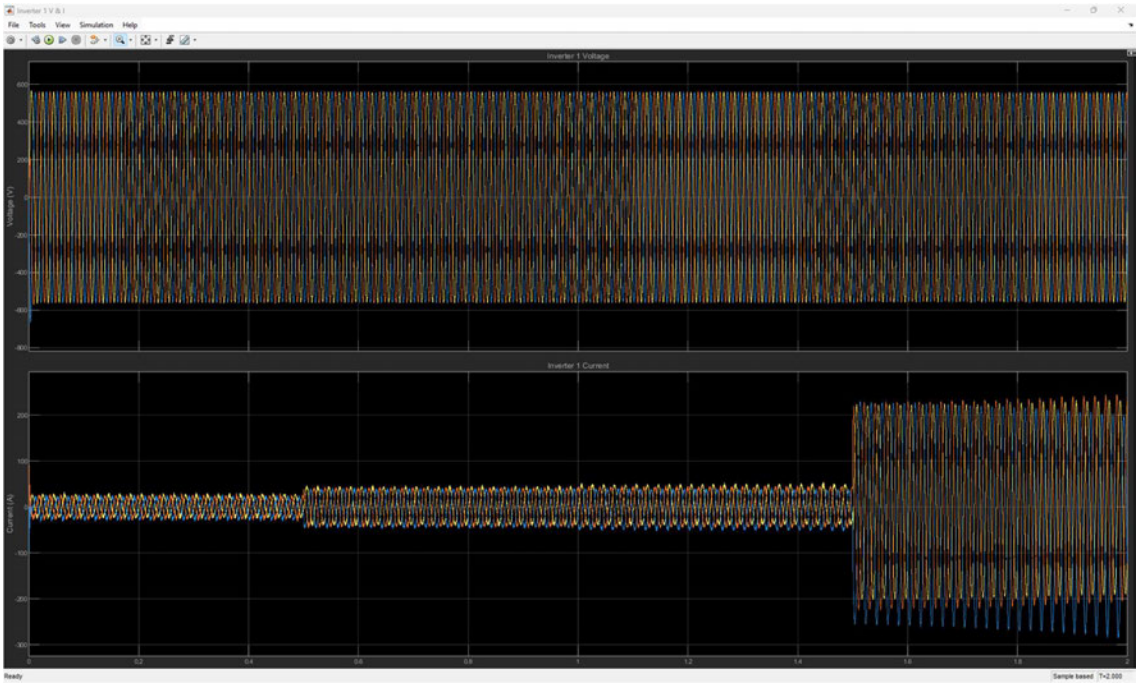

Figure 49 - Inverter 1 response to energise all in turn with added transformer and load at end of line

The 22kV voltage and current waveform shown in Figure 56 shows when Substation 2 is energised at t=1.5 seconds. There are no major transients, but the current drift can be seen.

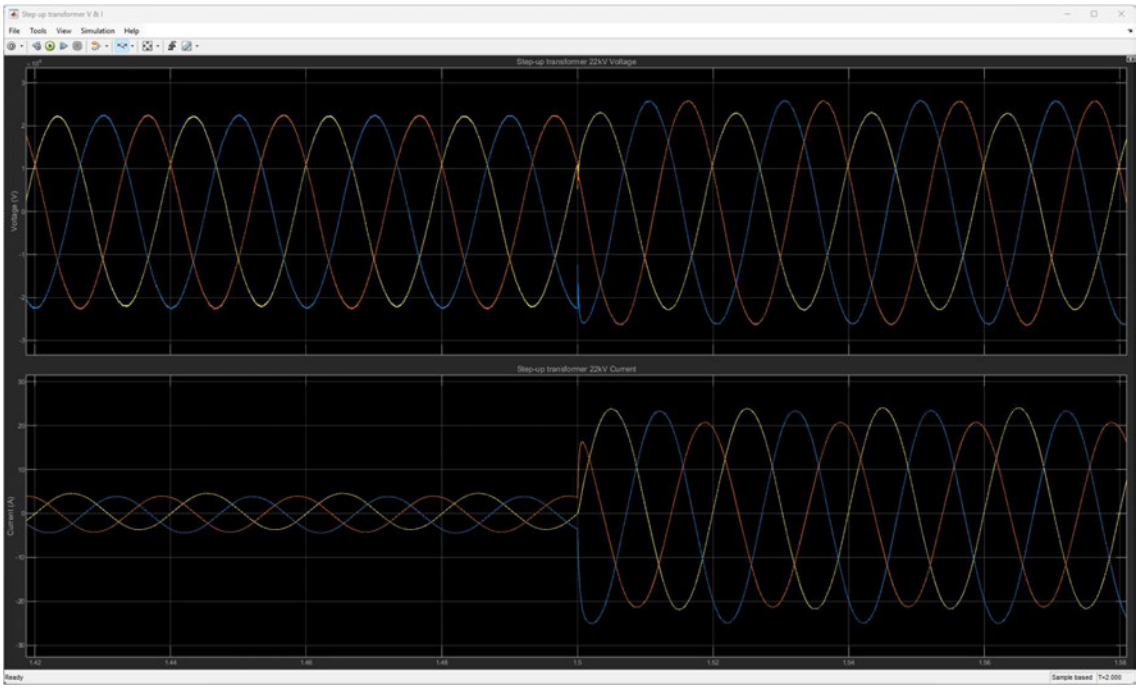

Figure 50 - 22kV side of Step-up transformer response

The issue becomes more apparent when looking at the 22kV power at Substation 1. The power fluctuations mentioned in Test Case 2 can be seen more clearly in Figure 58 below. The power fluctuations become more apparent when the sub transmission line is energised at t=1.0 seconds and increase when the second substation is energised at t=1.5 seconds. Due to the power fluctuations and current drift this test case is a fail.

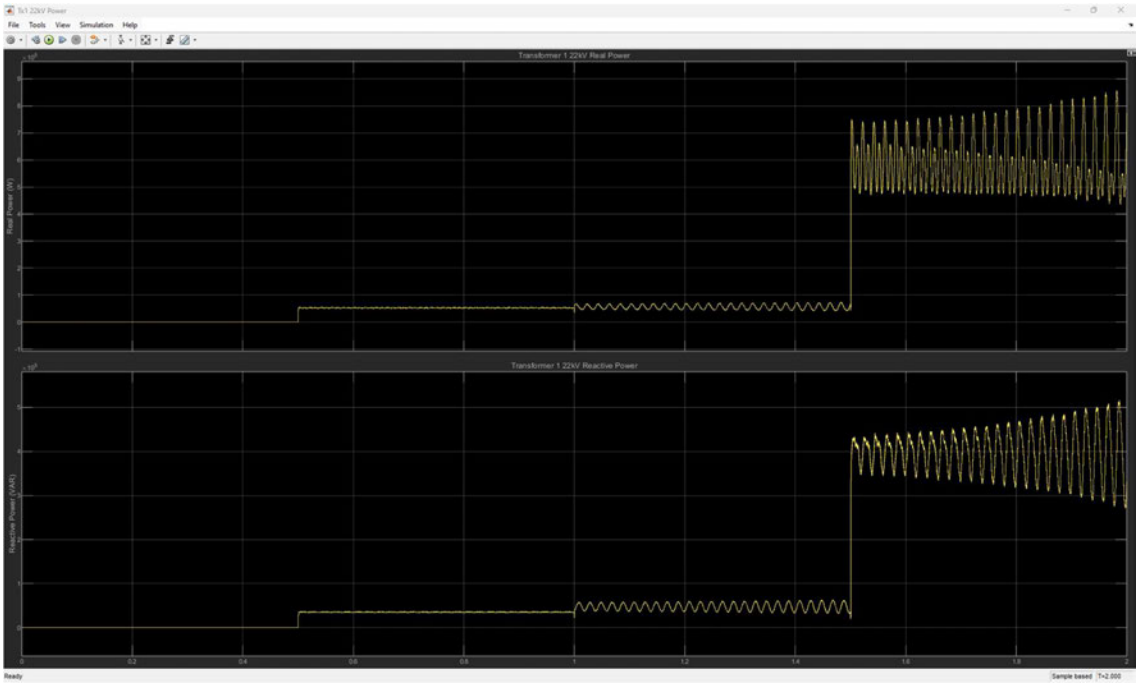

Figure 51 - 22kV Bus power

CHAPTER 5 CONCLUSION

The research conducted in this dissertation looked at understanding the existing and proposed generation sources of the Queensland Electricity Network. There is an increasing amount of DERs being connected to the network with many of these suitable to be used as a system restart service under the right conditions. GFMI control systems are varied with some more suited to enable the DERs to provide a reliable system restart service. The impacts of integration of non-synchronous generation to grid stability and reliability was not investigated in this research as that body of work was too large in scope to be included here.

Initial testing showed that a GFMI BESS was able to supply a resistive load. The inverters were shown to share the load with the voltage, current and frequency response remaining within the set point and statutory limits and remained stable.

When additional load was introduced to the system, energising a 66/22kV transformer, power fluctuations became noticeable. These power fluctuations continued to increase as more load, a short transmission line, was energised. Initial investigations failed to uncover the exact issue, but models including some of the improvements listed below should prove that DERs with Grid-forming capability can provide black restart services.

FUTURE WORK

Future work will include modification of the GFMI control system in the model to incorporate an Active Power Controller (APC) and Reactive Power Controller (RPC) as the primary controllers and a rerun of the test cases to check what improvements are gained.

Some research suggests the issue may be solved by moving from a voltage set point on the GFMI to an Adaptive Virtual Synchronous Generator (AVSG) as mentioned in Mohammed et.al (2024). The AVSG uses an APC and RPC as the primary controller and estimates the grid

impedance in real time which enables the GFMI to operate effectively under various grid conditions.

Once issues with the simulation of a GFMI connected to the Queensland Electricity Network are solved, an examination into the regulatory implications using GFMI BESS to create DRZs during an integrated black start can be done. This will involve discussions with AEMO, Transmission Network Service Providers (TNSP) and other DNSPs to ensure a coordinated approach can be achieved, and to explore the cost-effectiveness of using non-synchronous generation as a restart service.

With further research, data from simulations, and possible live tests of DRZs in Queensland, the black system restart time could be reduced. This will provide a benefit to all Queenslanders by reducing the amount of time that they are impacted by large-scale power outages.

References

AEMC 2016. *Fact Sheet: Black System Events.* Australian Energy Market Commission, Reliability Panel. Published 15 December 2016, viewed 2 February 2024 https://www.aemc.gov.au/sites/default/files/content/b705e0e4-afd3-47ef-bc41-32ea3393629c/Fact-Sheet-Black-system-events.pdf

Adeui, O, Marshall, B, 2020, Black Start from VSC HVDC and its impact on AC Protection Coordination, Webcast, February 2020, The National HVDC Centre, viewed 30 March 2024, https://www.hvdccentre.com/wp-content/uploads/2020/02/EPRI-HVDC-Restoration-Project-Final-Webinar_20200213.pdf

AEMO 2021a, *SRAS GUIDELINE, System Restart Ancillary Services*. Version 2.1. Australian Energy Market Operator. Published 8 February 2021. SRAS Guideline 2020 (aemo.com.au)

AEMO 2021b, Advanced Application of Grid-scale Inverters in the NEM – An Engineering Framework report on design capabilities needed for the future National Electricity Market, White Paper, August 2021, viewed 21 March 2024, https://aemo.com.au/-/media/files/initiatives/engineering-mohframework/2021/application-of-advanced-grid-scale-inverters-in-the-nem.pdf

AEMO 2023, Voluntary Specification for Grid-forming Inverters – A statement of voluntary threshold requirements and additional capabilities for inverters and other power electronic devices with grid-forming capability, May 2023, viewed 21 March 2024, https://aemo.com.au/-/media/files/initiatives/primary-frequency-response/2023/gfm-voluntary-spec.pdf?la=en&hash=F8D999025BBC565E86F3B0E19E40A08E

APA 2024, *Directlink | APA Group* (2024) *Directlink*, viewed 30 March 2024, https://www.apa.com.au/our-services/other-energy-services/electricity-interconnectors/directlink/

Asheibi, A & Shuaib, S 2019, 'A Case Study on Black Start Capability Assessment', *2019 International Conference on Electrical Engineering Research & Practice (ICEERP)*, Sydney, NSW, Australia, 2019, pp. 1-5. *https://doi.org/10.1109/ICEERP49088.2019.8956978*

Asensio, A.P, Gómez, S.A & Rodriguez-Amenedo, J.L, 2023. Black-start capability of PV power plants through a grid-forming control based on reactive power synchronization. *International Journal of Electrical Power & Energy Systems*, *146*, p.108730, https://doi.org/10.1016/j.ijepes.2022.108730

Aurecon 2021, *GPST Blackouts and System Restoration Research, Final Report,* Published 13 August 2021, CSIRO, Reference: 512363, Revision: 1A, viewed 12 September 2023, https://www.csiro.au/-/media/EF/Files/GPST-Roadmap/Topic-5-Blackouts-and-System-Restoration-Final-Report-with-alt-text-2.pdf

Aurecon 2023, *The Role of Inverter-Based Resources During System Restoration, Final Report,* 10 July 2023, CSIRO, Reference: P521937, Revision: 1, viewed 12 September 2023, https://www.csiro.au/-/media/EF/Files/GPST-Roadmap/Final-Reports/Topic-5-GPST-Stage-2.pdf

Cherevatskiy, S, Sproul, S, Zabihi, S, Korte, R, Klingenberg, H, Buchholz, B & Oudalov, A 2020, August. Grid forming energy storage system addresses challenges of grids with high penetration of renewables (a case study). In *Proc. CIGRÉ Session* (Vol. 2, p. 322), https://www.electranet.com.au/wp-content/uploads/2021/02/CIGRE48-Grid-Forming-BESS-Case-Study-August-2020.pdf

Dong, D, Wang, P, Qin, W & Han, X 2014, 'Investigation of a microgrid with vanadium redox flow battery storage as a black start source for power system restoration', *Proceedings of the 2014 IEEE 9th Conference on Industrial Electronics and Applications (ICIEA)*, Hangzhou, China, 9-11 June 2014, pp. 140-145, viewed 5 September 2023, https://doi.org/10.1109/ICIEA.2014.6931147

Dursun, M & Döşoğlu, MK 2018, 'LCL Filter Design for Grid Connected Three-Phase Inverter', in *2018 2nd International Symposium on Multidisciplinary Studies and Innovative Technologies (ISMSIT)*, IEEE, pp. 1–4.

Feldman, D & Oliviera, RV de 2021, 'Operational and control approach for PV power plants to provide inertial response and primary frequency control support to power system black-start', *International Journal of Electrical Power & Energy Systems*, Volume 127, p.106645, viewed 14 September 2023, https://doi.org/10.1016/j.ijepes.2020.106645

Gracia, J, O'Connor, P, Markel, L, Shan, R, Rizy, D & Tarditi, A 2019, *Hydropower Plants as Black Start Resources*, Hydrowires, US Department of Energy, https://www.energy.gov/eere/water/articles/hydropower-plants-black-start-resources

IEEE 2020, *IEEE Guide for Synchronous Generator Modeling Practices and Parameter Verification with Applications in Power System Stability Analyses*, in IEEE Std 1110-2019 (Revision of IEEE Std 1110-2002) , vol., no., pp.1-92, 2 March 2020, https://10.1109/IEEESTD.2020.9020274

Izadkhast, S, Cossent, R, Frías, P, García-González, P & Rodrígez-Calvo, A 2022, *Performance Evaluation of a BESS Unit for Black Start and Seamless Islanding Operation*, Energies 2022, 15, 1736. https://doi.org/10.3390/en15051736

Jain, H, Seo, G, Lockhart, E, Gevorgian, V, and Kroposki, B 2020, 'Blackstart of Power Grids with Inverter-Based Resources', *2020 IEEE Power & Energy Society General Meeting (PESGM)*, Montreal, QC, Canada, 2020, pp. 1-5, viewed 8 September 2023, *https://doi.org/10.1109/PESGM41954.2020.9281851*

Li, J, You, H, Qi, J, Kong, M, Zhang, S & Zhang, H 2019, *Stratified Optimization Strategy Used for Restoration With Photovoltaic-Battery Energy Storage Systems as Black-Start Resources,* IEEE Access, vol. 7, pp. 127339-127352, 2019, viewed 9 September 2023, https://doi.org/10.1109/ACCESS.2019.2937833

Lin, Y., Eto, J.H., Johnson, B.B., Flicker, J.D., Lasseter, R.H., Villegas Pico, H.N., Seo, G.S., Pierre, B.J. and Ellis, A., 2020. *Research roadmap on grid-forming inverters* (No. NREL/TP-5D00-73476). National Renewable Energy Lab.(NREL), Golden, CO (United States), viewed 30 March 2024, https://doi.org/10.2172/1721727

Liu, W & Liu, Y 2019, 'Enabling wind farm to be black-start source by energy storage', The Journal of Engineering, 2019, viewed 9 September 2023, https://doi.org/10.1049/joe.2018.9302

Liu, Z, Liu, J and Zhao, Y 2014. *A Unified Control Strategy for Three-Phase Inverter in Distributed Generation*, IEEE TRANSACTIONS ON POWER ELECTRONICS, VOL. 29, NO. 3, MARCH 2014, https://doi.org/10.1109/TPEL.2013.2262078

MATLAB 2024a, abc to dg0, dq0 to abc, *Perform transformation from three-phase (abc) signal to dq0 rotating reference or the inverse*, https://www.mathworks.com/help/releases/R2024a/sps/powersys/ref/abctodq0dq0toabc.html

MATLAB 2024b, Synchronous Machine pu Standard*, Model dynamics of three-phase round-rotor or salient-pole synchronous machine using standard parameters in pu units,* https://www.mathworks.com/help/releases/R2024a/sps/powersys/ref/synchronousmachinepustandard.html#mw_b29404d2-51fe-470c-9816-942163ced755

Modi, N, Mock, C and Christiansen, C 2023, *Australian landscape of grid-forming batteries*, *ESIG*, viewed 29 March 2024, https://www.esig.energy/australian-landscape-of-grid-forming-batteries/

Mohammed, N, Udawatte, H, Zhou, W, Hill, D and Bahrani, B 2024, Grid-Forming Inverters: A Comparative Study of Different Control Strategies in Frequency and Time Domains, *IEEE Open Journal of the Industrial Electronics Society*, viewed 26 September 2024, https://doi.org/10.1109/OJIES.2024.3371985

National Grid ESO 2019, *Black start from non-traditional generation technologies. Technology Capability and Readiness for Distribution Restoration,* Released June 2019, viewed 3 February 2024, https://www.nationalgrideso.com/document/148201/download

National Grid ESO 2023a, *Distributed Restart. Power Engineering and Trials. Demonstration of Black Start from DERs (Live Trial Report). Part 3 – October 2023,* Released 9 October 2023, viewed 9 October 2023, https://www.nationalgrideso.com/document/289876/download.

National Grid ESO 2023b, *Distributed Restart. Energy Restoration for Tomorrow. Final Findings and Proposals for Electricity System Restoration from DERs – October 2023,* Released 11 October 2023, viewed 11 October 2023, https://www.nationalgrideso.com/document/271831/download.

Pagnani, D, Blaabjerg, F, Bak, C, Faria da Silva, F, Kocewiak, L, & Hjerrild, J 2020a, *Offshore Wind Farm Black Start Service Integration: Review and Outlook of Ongoing Research*, Energies 2020, 12(23), 6286, viewed 25 September 2023, https://doi.org/10.3390/en13236286

Pagnani, D, Kocewiak, L, Hjerrild, J, Blaabjerg, F, and Bak, C 2020b, 'Overview of Black Start Provision by Offshore Wind Farms', *IECON 2020 The 46th Annual Conference of the IEEE Industrial Electronics Society*, Singapore, 2020, pp. 1892-1898, viewed 18 September 2023, https://doi.org/10.1109/IECON43393.2020.9254743

Queensland Department of Energy and Public Works (2021), Electricity Generation MAP – Department of Energy and Public Works, QLD, Power plants map of Queensland, viewed 20 March 2024, https://electricity-generation-map.epw.qld.gov.au/

Rathnayake, D.B., Akrami, M., Phurailatpam, C., Me, S.P., Hadavi, S., Jayasinghe, G., Zabihi, S. and Bahrani, B., 2021. Grid forming inverter modeling, control, and applications. *IEEE Access*, *9*, pp.114781-114807, viewed 25 March 2023, https://doi.org/10.1109/ACCESS.2021.3104617

Roscoe, A, Knueppel, T, Da Silva, R, Brogan, P, Gutierrez, I, Elliott, D & Perez Campion J, 2021, "Response of a grid forming wind farm to system events, and the impact of external and internal damping", IET Journals, published2021, https://doi.org/10.1049/iet-rpg.2020.0638

Smith, C, Gargoom, A, Arif, M.T & Haque, M.E 2022, 'Control Techniques for Grid Forming Inverters: A Comparative Analysis' In *2022 IEEE Industry Applications Society Annual Meeting (IAS)* (pp. 1-9). IEEE, https://doi.org/10.1109/IAS54023.2022.9939796

Sun, W, Liu, C & Liu, S 2011, 'Black Start Capability Assessment in Power System Restoration', *2011 IEEE Power and Energy Society General Meeting*, Detroit, MI, USA, 2011, pp. 1-7, viewed 13 September 2023, https://doi.org/10.1109/PES.2011.6039752

Tongge, L, Yonghong, H, Junyi, M & Yimin, X 2020, 'The Research on Black Start Strategy of Distributed Photovoltaic-Battery Energy Storage Systems Based on Cluster Division', *2020 IEEE Sustainable Power and Energy Conference (iSPEC),* Chengdu, China, 2020, pp. 337-342, viewed 27 September 2023, *https://doi.org/*10.1109/iSPEC50848.2020.9351025

Unruh, P., Nuschke, M., Strauß, P. and Welck, F., 2020. Overview on grid-forming inverter control methods. *Energies*, *13*(10), p.2589, viewed 26 March 2024, https://doi.org/10.3390/en13102589

Zhu, Y, Sutanto, D & Morrison, I 1991, 'Graphic-assisted expert system for power system black restart', *1991 International Conference on Advances in Power System Control, Operation and Management, APSCOM-91*, Hong Kong, 1991, pp. 514-517 vol.2, viewed 29 September 2023, https://ieeexplore.ieee.org/document/154126

APPENDIX A

Other inverter responses during test case 1.

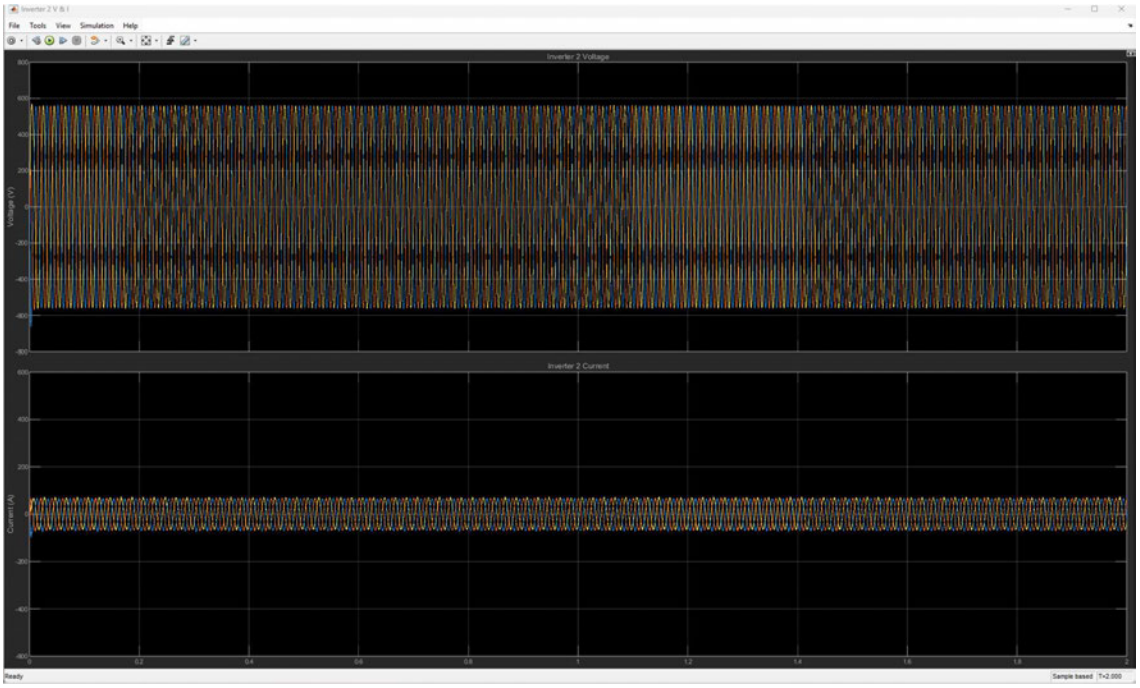

Figure 52 - Inverter 2 Voltage and Current

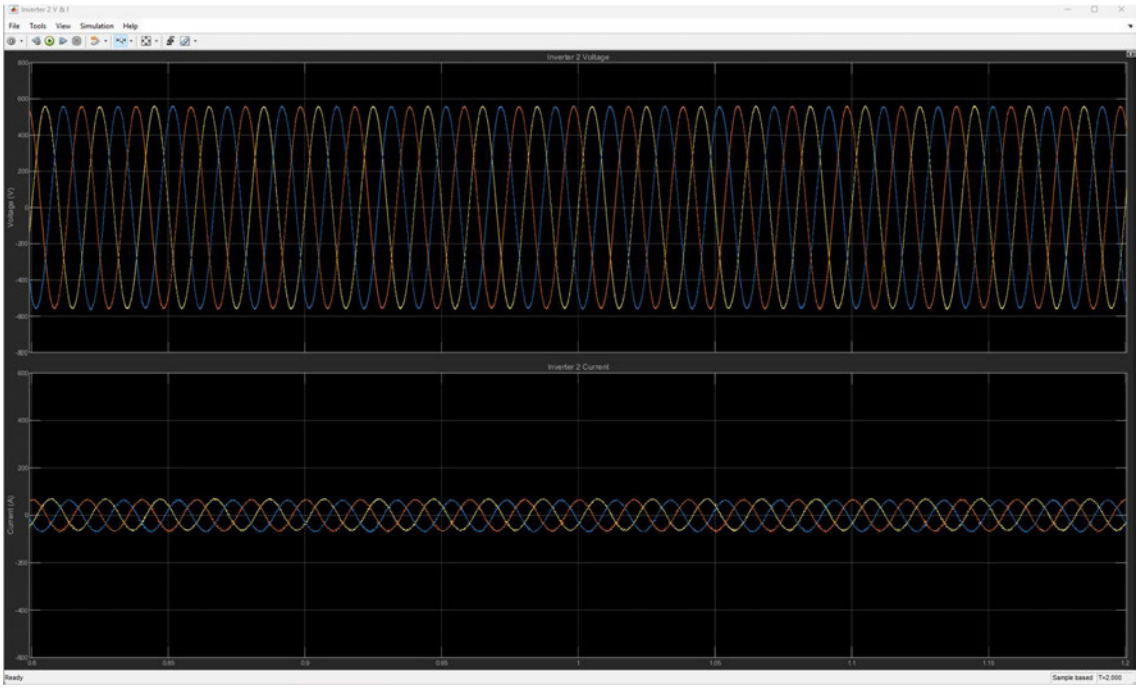

Figure 53 - Inverter 2 Voltage and Current between t=0.8 seconds and t= 1.2 seconds

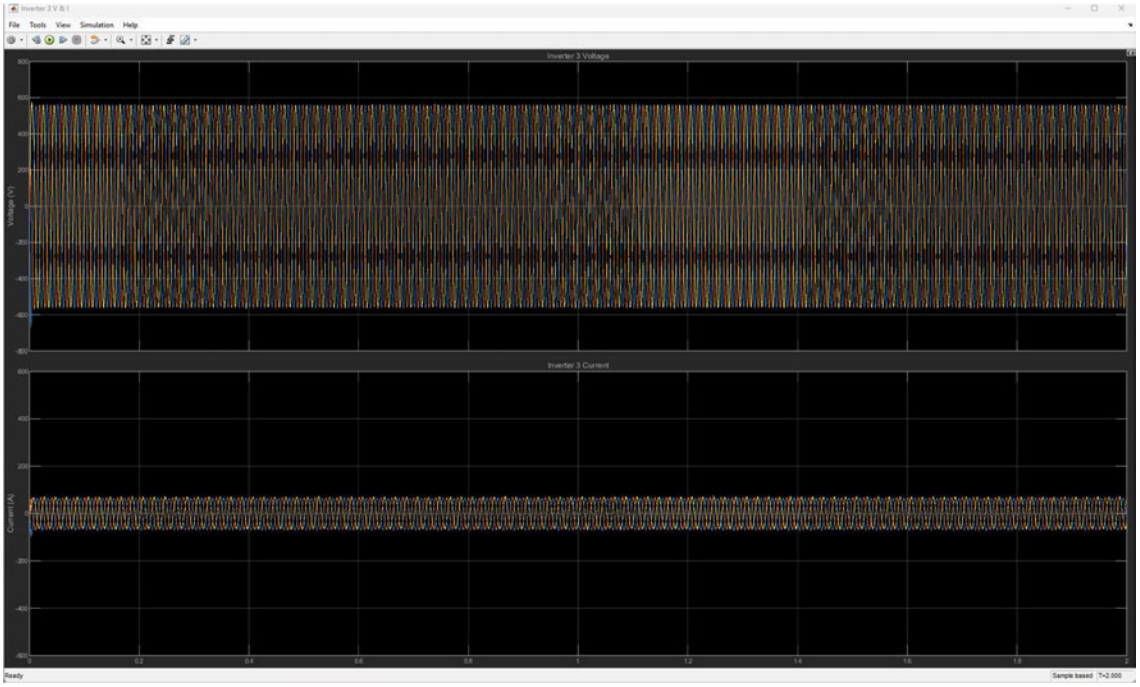

Figure 54 - Inverter 3 Voltage and Current

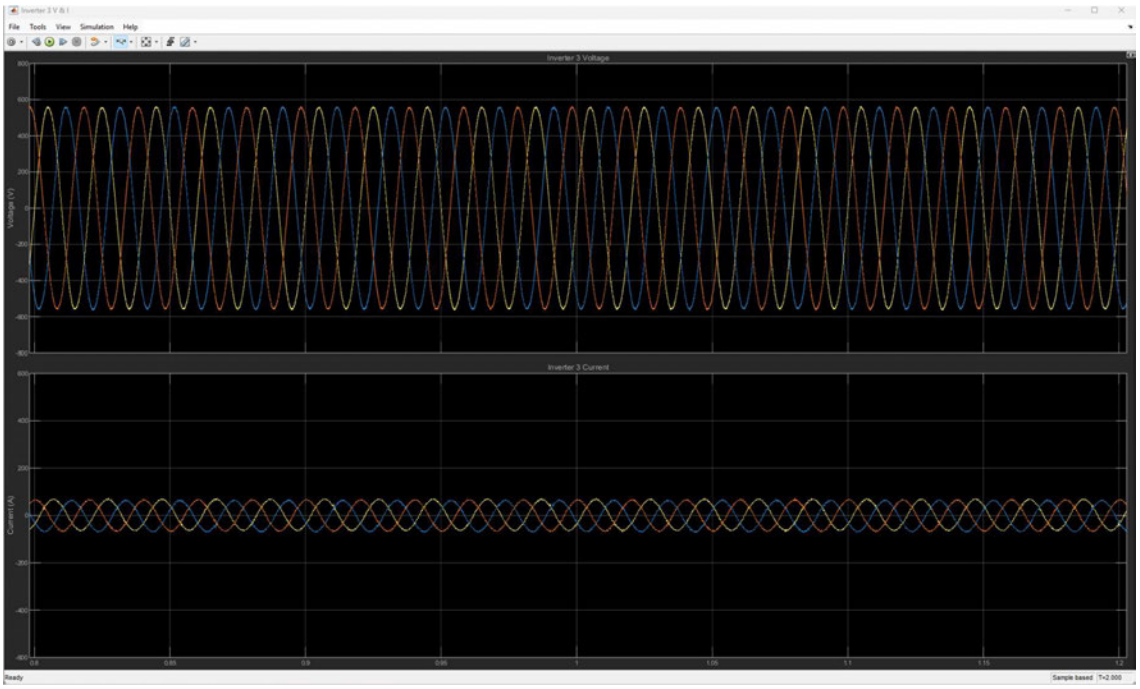

Figure 55 - Inverter 3 Voltage and Current between t=0.8 seconds and t=1.2 seconds

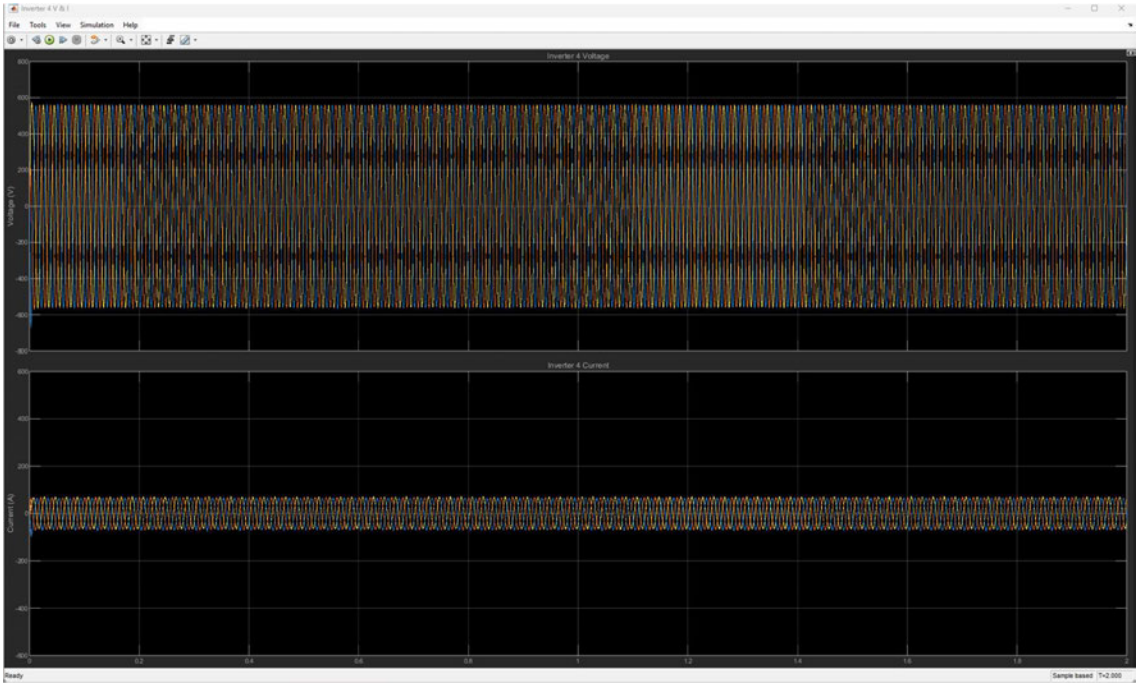

Figure 56 - Inverter 4 Voltage and Current

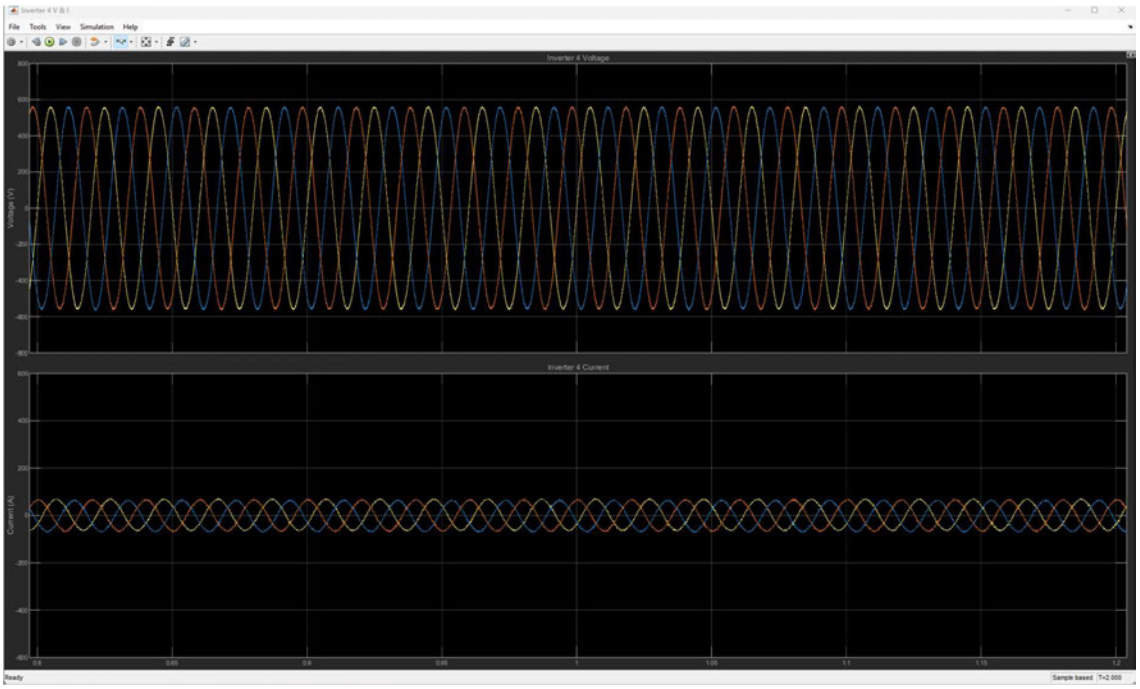

Figure 57 - Inverter 4 Voltage and Current between t=0.8 seconds and t=1.2 seconds

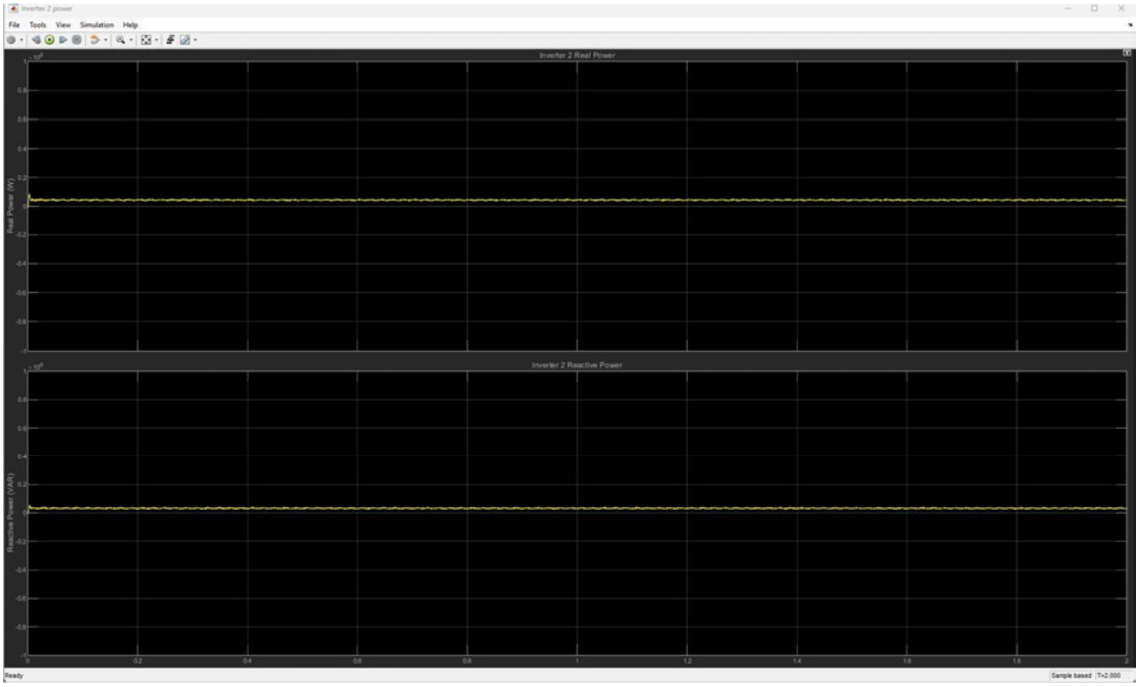

Figure 58 - Inverter 2 Power. Scaled to full power output

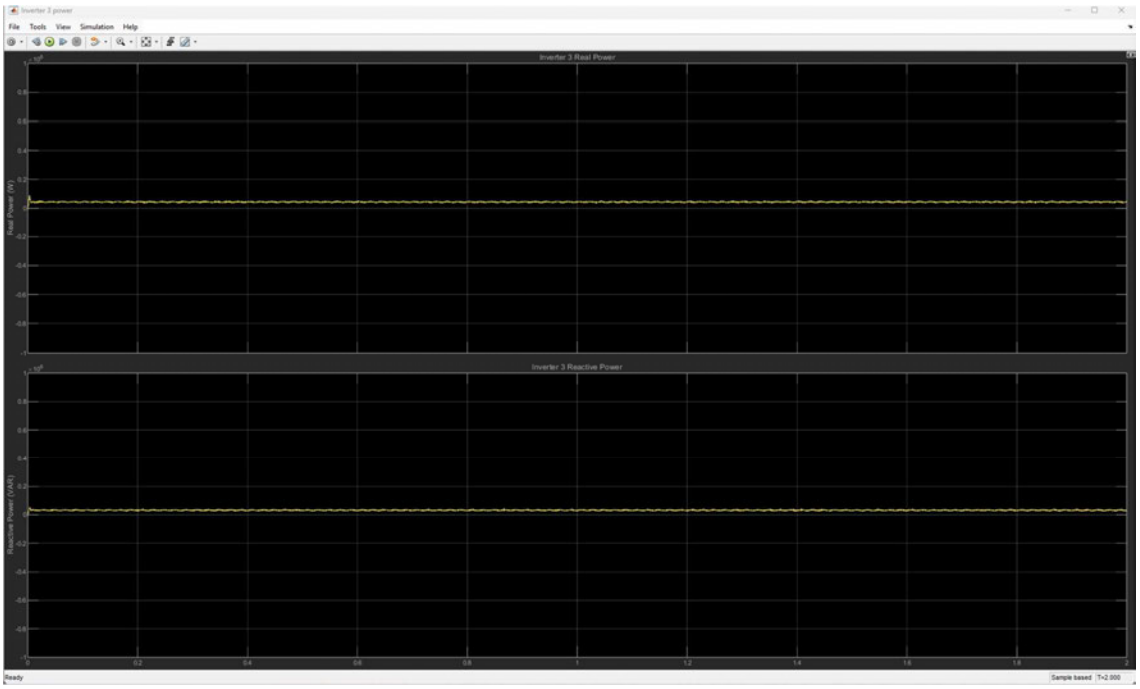

Figure 59 - Inverter 3 Power. Scaled to full power output

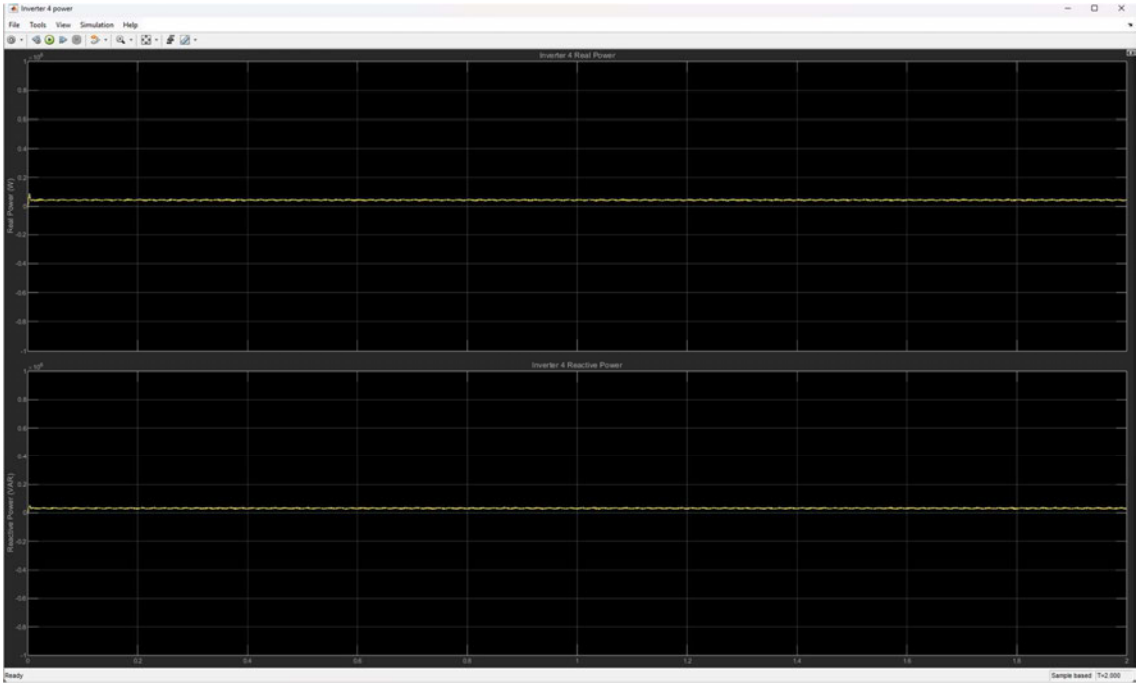

Figure 60 - Inverter 4 Power. Scaled to full power output

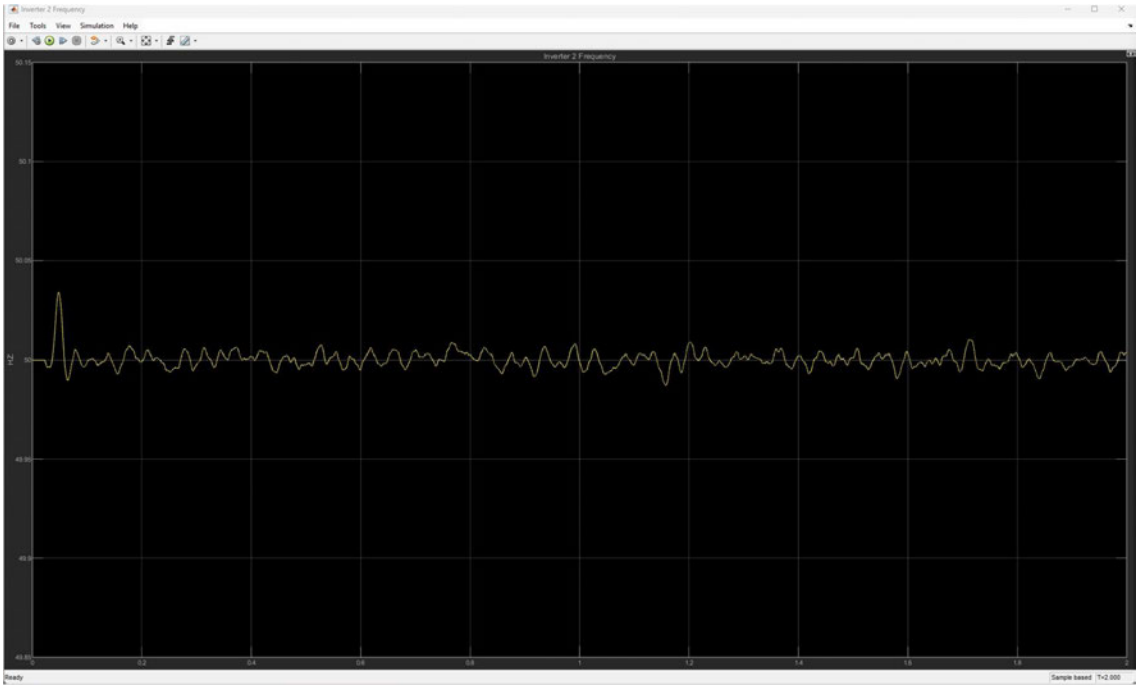

Figure 61 - Inverter 2 frequency response

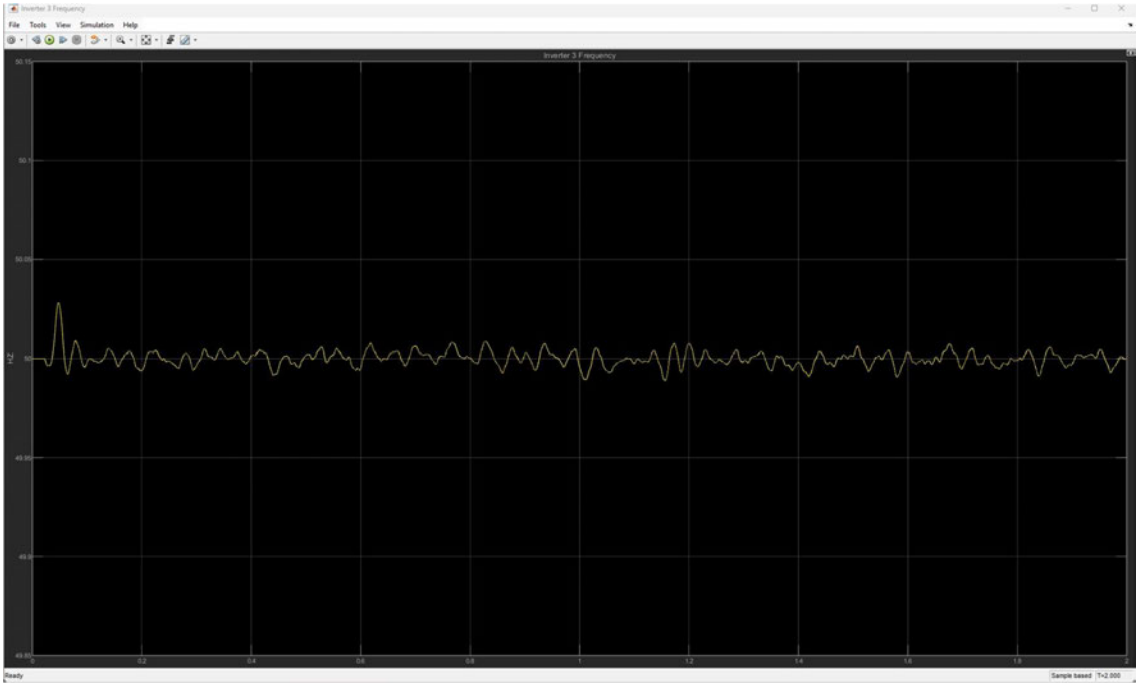

Figure 62 - Inverter 3 frequency response

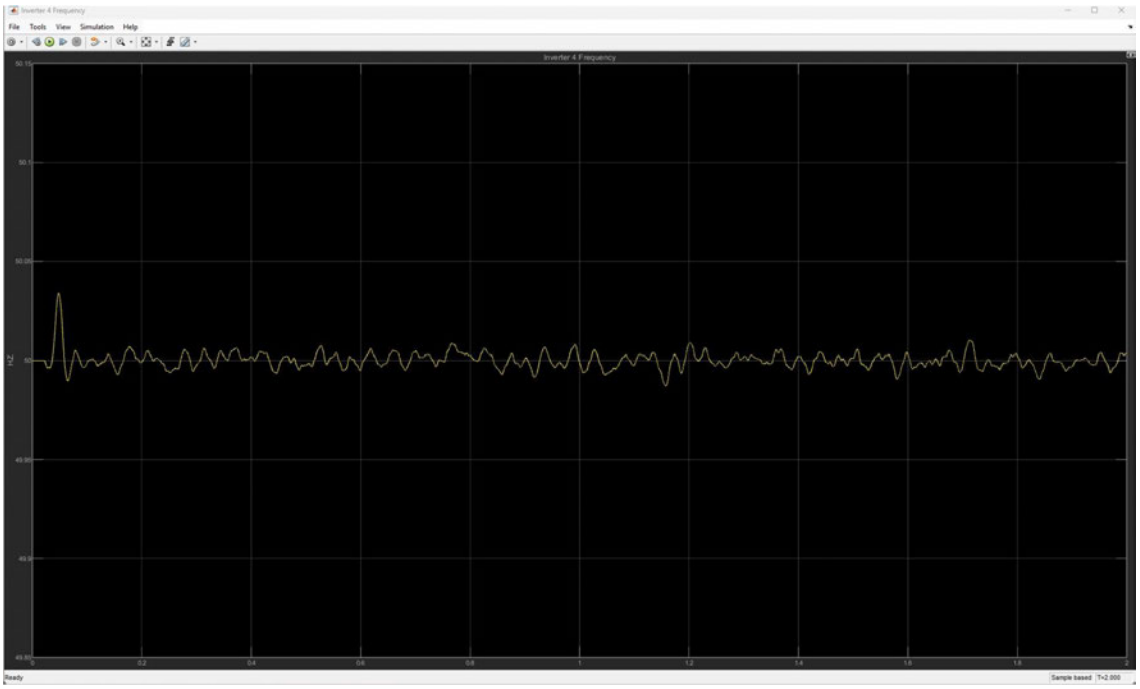

Figure 63 - Inverter 4 frequency response

APPENDIX B

Appendix B contains the equations to calculate LCL filter size for IBRs.

$$S = \frac{P}{pf} \tag{19}$$

$$I = \frac{S}{V_p} \tag{20}$$

$$Z_b = \frac{{V_p}^2}{P} \tag{21}$$

$$C_b = \frac{1}{2 * \pi * f_g * Z_b} \tag{22}$$

$$I_{max} = \frac{P * \sqrt{2}}{V_p} \tag{23}$$

Where

Z_b is the base impedance

V_p is the RMS phase voltage

C_b is the base capacitance

V_p is the phase voltage

pf is the power factor

f_g is the grid frequency

If the rated current is allowed to fluctuate by 10%

$$\Delta I_{L\_max} = 0.1 * I_{max} \quad (24)$$

$$L_1 = \frac{V_p}{16 * f_{sw} * \Delta I_{L\_max}} \quad (25)$$

Where

L_1 is the inverter side inductance

f_{sw} is the switching frequency

$$C_f = 0.05 * C_b \quad (26)$$

$$L_2 = 0.6 * L_1 \quad (27)$$

Where 0.6 is the ratio of L_1 to L_2 and

C_f is the filter capacitance

L_2 is the grid side inductance

$$\omega_{res} = \sqrt{\frac{L_1 + L_2}{L_1 * L_2 * C_f}} \quad (28)$$

$$f_{res} = \frac{\omega_{res}}{2\pi} \quad (29)$$

Where

ω_{res} is the resonance frequency of the filter in rad/s

f_{res} is the resonance frequency on the filter in Hz

To reduce some of the ripple at the switching frequency, a resistor is placed in series with the filter capacitor.

$$R_f = \frac{1}{3 * C_f * \omega_{res}} \qquad (30)$$

Where

R_f is the damping resistance